Dispersive interactions for strong atom-photon coupling in guided nanophotonic fiber geomertry

CQuIC, UNM, Albuquerque, NM 87131, USA

(Dated: March 5, 2015)

Abstract

We analyze the tensor interaction of atoms and quantized modes of the electromagnetic field in the presence of a guiding nanophotonic optical fiber. When detuned from resonance, the tensor linear response yields phase shifts and polarization transformations conditional on the atomic spin. Such interactions can lead to strong entanglement between the collective atomic spin and the guided photonic modes with a few thousand atoms, even in a regime where Γ_{1D}, the rate of spontaneous emission into the guided mode, is not much larger than the free space Γ. We apply this to study QND measurement-induced squeezing of the pseudospin associated with the clock transition of atomic cesium, as well as squeezing of the physical atomic spin for applications in magnetometry. We find x dB of squeezing.

I. INTRODUCTION

Strong coupling between atoms and traveling photons is a prerequisite for quantum information processing protocols ranging from quantum-limited metrology to quantum communication and computation [1, 2]. A strong coupling strength of the photon-atom interaction can be achieved through shining light on-resonance with the atoms. The atoms, however, are highly excited in this process and emit photons as spontaneous emissions which may produce losses and decoherence. Various photonic structures including optical cavities [3, 4] and nanostructured waveguides [5, 6] have been developed to enhance the Purcell effect and to guide the spontaneous emission into the desired photonic modes. For instance, a photonic waveguide designed for near-resonance interaction requires a careful design to have a high ratio of Γ_{1D}/Γ, where Γ_{1D} is the decay rate into the guided modes while Γ is the total decay rate of an atom. Other drawbacks? How about heating and trapping challenges?

On the other hand, a strong photon-atom interaction can also be achieved in the dispersive regime when optical depth (OD) is large. In this regime, the atoms are almost sitting in the ground state and experiencing adiabatic dynamics in response to the interaction from a low-saturating photonic mode. Therefore, even if Γ_{1D}/Γ is small, the loss due to the spontaneous emission could be very low compared to the near-resonance atomic response regime. To achieve a large OD in free space, a large ensemble of trapped atoms is required. The optical depth can be expressed as $OD = N_e \frac{\sigma_0}{A}$, where N_e is the effective number of interacting atoms and is usually less than the actual number of trapped atoms due to mode mismatch, σ_0 is the atomic resonant cross section, and A is the mode area of the probe light. The effective atom number is determined by the mode volume and is positively correlated with the mode area for a Gaussian probe beam. Therefore, it is challenging to achieve a high OD [7].

In the last decade, subwavelength-diameter nanofibers have been theoretically proposed and experimentally demonstrated to be an efficient platform to realize the strong interaction between atoms and a traveling photon package [8–16]. On a typical nanofiber platform, alkali atoms can be trapped and laser-cooled on one side or two sides of a fiber waveguide to form a 1D-lattice using a two-color evanescent light field. A guided probe light with or without a pumping light field can then be used to implement various quantum metrology and quantum information protocols benefited from the strong atom-photon interactions. There are many

advantages of using the nanofiber platform compared to the free space interface. One such advantage is that the evanescent field where the atoms are sitting at could be much stronger, and hence the effective mode area per atom becomes dramatically smaller, which is inversely proportional to the normalized mode square at the atom positions. Another advantage is that all atoms are experiencing the same strength of optical field and the scattered fields from the atoms can be well matched to the guided modes, and hence the effective number of atoms equals the actual number of trapped atoms and is no longer correlated with the effective mode area. As we will show later in this paper for this resulted strong interaction, only 2000 atoms are needed surrounding a $450nm$-diameter nanofiber to achieve an OD of 200 compared to millions of atoms needed in a typical free-space configuration.

So far, a lot of attentions have been casted to the near-resonance regime using a guided probe light on a waveguide platform to tame the spontaneous emission and photon scattering nature of the process [17–28]. While in the dispersive regime, few dedicated theoretical frameworks have been drawn, yet promising experiments conducted by Dawkins, Béguin and others have shown that a far-off-resonance probe light can be used to estimate the number of atoms trapped surrounding a nanofiber in a high resolution without destruct the state of the atoms [14, 29]. In principle, one could use the general theory of light-atom interaction developed for waveguides to guide the design of the dispersive quantum interface in nanofibers. However, it may become confusing when one read over those theories derived in various methods and emphasized on different aspects. In this work, we have derived the dispersive interaction theory for the nanofiber platform in various methods and make connections between them. To better implementing atom-photon entanglement, spin squeezed states and some other quantum information processing (QIP) resources, we will basically employ the one-color probe setup introduced in [14] with a homodyne measurement to the output light (see Fig. 1) in stead of the two-color probe setup presented in [29] which should be a combination of two probe channels. We will show that the simple setup can achieve a precise enough atom number estimation with quantum nondemolition (QND) measurement. We restrict our attention to a single-mode nanofiber system coupling to cesium atoms in the dispersive regime and calculate the phase shift and transformation of polarization of the guided modes and some specific tasks, but the theory itself can be easily generalized to analyze much general waveguide-atom interface applications including spin squeezing via QND measurements [30, 31], quantum memories [32–36], quantum data

bus and other QIP applications [37] which have been considered for the free space or other platform trapped atomic systems.

The consequent parts of this paper are organized as follows. We first overview the light-atom interaction in dyadic Green function method and the input-output formalism in Heisenberg picture to derive the phase shift and birefringence effect of the guided fields. Then we will compare the nanofiber performance to the free space case to obtain the relative enhancement factors. We apply our theory to polarization spectroscopy measurements using the clock states of the cesium atoms and spin squeezing technique. The sensitivity of atom number estimation through the dispersive interaction will be discussed as an example. We will conclude our work at the end.

II. PHASE SHIFT AND POLARIZATION TRANSFORMATION OF THE GUIDED MODES OF A NANOFIBER IN PRESENCE OF AN ATOM

The light-atom interaction Hamiltonian can be defined in terms of the atomic angular momentum operator $\hat{\mathbf{F}}$ and the photonic Stokes vector operator $\hat{\mathbf{S}}$ [31]. For instance, the evolution operator of a Faraday interaction can be given by

$$\hat{U}(\tau) = e^{i\chi \hat{S}_3 \cdot \hat{F}_z}. \tag{1}$$

Suppose the initial state of the atom-light system is given by

$$|\Psi(0)\rangle = \frac{1}{\sqrt{2}}(|\uparrow\rangle + |\downarrow\rangle)|\phi_L\rangle \tag{2}$$

where the atom is prepared in a superposition of spin up and down state, and the light in prepared in an arbitrary $|\phi_L\rangle$ state. The output after the Faraday interaction of duration τ will become

$$|\Psi(\tau)\rangle = \frac{1}{\sqrt{2}} \left[|\uparrow\rangle e^{+i\chi \hat{S}_3} |\phi_L\rangle + |\downarrow\rangle e^{-i\chi \hat{S}_3} |\phi_L\rangle \right] \tag{3}$$

$$= \frac{1}{\sqrt{2}} \left[|\uparrow\rangle |\phi_L^1\rangle + |\downarrow\rangle |\phi_L^2\rangle \right] \tag{4}$$

The polarization of the light has been rotated along the z-axis, either $+2\chi$ or -2χ around the S_3 axis on the Poincare sphere entangled with the spin state. Now the state of the joined system is in an entangled state between the spin system and the light. The entanglement
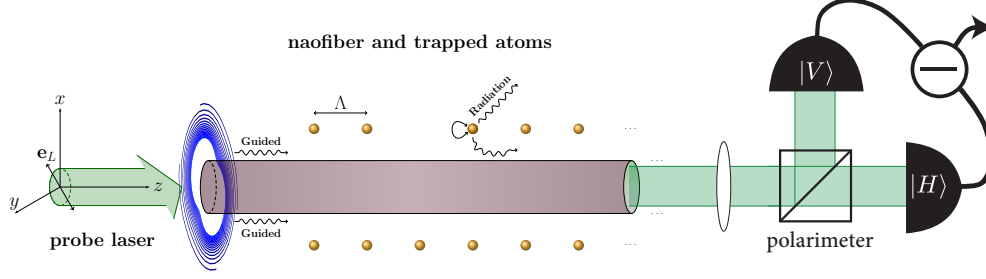
FIG. 1: Birefringence measurement setup for a nanofiber trapped atomic system. In the evanescent field of the nanofiber, atoms (golden balls) randomly occupy the periodic trapping sites on both sides of a 1D-chain with a period of Λ.

between the atomic system and the light can be employed for quantum metrology and quantum information processing.

The Faraday effect does not change the helicity of the polarized light. In general, however, the output Stokes vector $\mathbf{S}_{out}$ can be an arbitrary rotation along the three Poincare sphere axis after the atom-light interaction:

$$\mathbf{S}_{out} = \mathbf{S}_{in} + \mathbf{\Theta} \times \mathbf{S}_{in}, \tag{5}$$

where the rotation angle along the i-axis is $\Theta_i \propto N_A \left(\frac{\sigma_0}{A} \right) \left(\frac{}{2} \right)$ with effective atom number N_A, on-resonance scattering cross section σ_0, effective mode area A which is inversely proportional to the mode square of the normalized electric field, atomic decay rate Γ and the detuning Δ. The rotation along the S_1 or S_2 axes yields the birefringence effect for the light.

Missing figure

Maybe a figure to show the Poincare sphere and the Faraday/birefringence effects here.

For a given detuning and atom species, the effective atom number, N_A, and the optical depth per atom, $OD = \sigma_0/A$, determines the rotation angle and hence the coupling strength between the joint systems. There have been a huge amount of efforts to enhance the atom-light interaction strength using the atom trapping configuration in free-space or

5

vacuum [Refs]. The problem for the vacuum trapping configuration is that the effective atom number N_A is positively correlated with the effective mode area, and hence the total optical depth, $N_A \left(\frac{\sigma_0}{A} \right)$, is limited to some finite value around $50 \sim 100$, typically with 10^6 atoms. The nanofiber trapped atomic system, however, decouples the correlation between the effective atom number and the effective mode area. Each atom has the same amount of effective mode area, and experiences the same strength of field. Moreover, the evanescent probing field of the nanofiber where the atoms are trapped can be very strong compared to the vacuum trapping configuration due to the weak confinement of the nanofiber with a sub-wavelength diameter. With about 2000 atoms, it is possible to achieve a total optical depth of 200 as will be shown later. All of these factors above makes the nanofiber a promising platform for atom-light interfaces with strong coupling strength.

In the consequent sections, we will firstly employ the Green function method to solve the semi-classical radiation and scattering problem of a two-level dipole in the evanescent field of a nanofiber. Then we will extend to the real atom in a quantized field case. The phase shift and birefringence effects will be studied in terms of orthogonal field components. For example, if the input field is diagonally linearly polarized as

$$\mathbf{E}_{in} = E_0(\hat{e}_x + \hat{e}_y), \tag{6}$$

the output field can be written as

$$\mathbf{E}_{out} = E_0(t_x e^{i\phi_x} \hat{e}_x + t_y e^{i\phi_y} \hat{e}_y). \tag{7}$$

The ratio of the attenuation coefficients, t_x and t_y, indicates the helicity of the polarization of the light. ϕ_x and ϕ_y represent the phase shifts in the x- and y-modes. We will consider the phase shift for one input mode first, and then present our theory for the birefringence effect with two orthogonal input modes.

A. Nano ber mode scattering due to an atom using the dyadic Green function method

The radiation from N_A atoms in the evanescent field of a nanofiber obeys the Maxwell equation given by

$$\left[-\nabla \times \nabla \times + n^2(\mathbf{r}) \frac{\omega^2}{c^2} \right] E(\mathbf{r}) = -4\pi \frac{\omega^2}{c^2} \ (\mathbf{r}) \cdot E(\mathbf{r}) = -4\pi \frac{\omega^2}{c^2} \sum_{\mathbf{r}'} \delta(\mathbf{r} - \mathbf{r}') \ (\mathbf{r}') \cdot E(\mathbf{r}), \tag{8}$$

6

where the atoms are treated as electric dipole sources positioned at $\mathbf{r}'$ on the right-hand-side of the equation. We denote $E(\mathbf{r})$ as the electric field, $\chi(\mathbf{r})$ as the electric susceptibility and $\alpha(\mathbf{r}')$ as the polarizability due to the dipole source at $\mathbf{r}'$. In this paper, we first only consider the radiation from one atom, and then the many-atom case will be naturally extended in

is called a radiation mode. There are finite guided modes with discrete β values for a given nanofiber; radiation modes, however, have continuous β and are countless. Correspondingly, the dyadic Green function can be decomposed into guided mode components and radiation mode components.

One can also use the eigenmode expansion method [41, 42] to expand the Green functions in terms of bare-fiber modes. For our problem, we only care about the guided mode contributions which are the dominant components detected at the end of a long nanofiber. We use single mode fibers for this study. The only allowed guided mode for a single-mode fiber is called HE_{11} mode which has degeneracies of two propagating directions and two polarization patterns. The propagation constant β_0 is fixed once the wavelength and the geometry of the nanofiber are given. One can show that the dyadic Green function for the guided modes can be written as [42]

$$\mathbf{G}_g(\mathbf{r}, \mathbf{r}') = -\frac{i n_g}{2 k_0} \sum_{m, f = \pm 1} \mathbf{u}^{(\mu)}(r_\perp) \mathbf{u}^{(\mu)}(r_\perp') e^{i f \beta_0 (z - z') + i m (\phi - \phi')} \tag{14}$$

$$= -\frac{i n_g}{2 k_0} \sum_{m, f = \pm 1} \mathbf{u}^{(\mu)}(r_\perp) \mathbf{u}^{(\mu)*}(r_\perp') e^{i f \beta_0 (z - z') + i m (\phi - \phi')}. \tag{15}$$

In the equation above, the wave number $k_0 = \frac{\omega_0}{c}$ for a given angular frequency ω_0, and the transverse modes of the nanofiber, $\mathbf{u}^{(\mu)}(\mathbf{r})$, are defined by

$$[-\nabla \times \nabla + \frac{\omega_0^2}{c^2} n^2(\mathbf{r})] \mathbf{u}^{(\mu)}(\mathbf{r}) = 0, \tag{16}$$

where the mode index $\mu = (\beta_0, m, f)$ with angular moment quantum number m and propagation index f. The adjoint mode index $\tilde{\mu} = (\beta_0, -m, -f)$ and we have defined the or-

the output field can be expanded in terms of the guided fiber modes as

$$\mathbf{E}(\mathbf{r}) = E_0 \mathbf{u}_{(\beta_0,1,1)}(\mathbf{r}) + \sum_{m,f=\pm 1} C_{mf} E_0 \mathbf{u}^{(\beta_0,m,f)}(\mathbf{r}), \tag{18}$$

where the mode projection coefficients are

$$C_{mf} = -4\pi k_0^2 \alpha \int d^2 r_\perp n^2(\mathbf{r}_\perp) \mathbf{u}^{(\beta_0,m,f)*}(\mathbf{r}) \cdot \mathbf{G}^g(\mathbf{r},\mathbf{r}') \cdot \mathbf{u}^{(\beta_0,1,1)}(\mathbf{r}'). \tag{19}$$

Using the eigenmode expansion of the dyadic Green function, these coefficients become

$$C_{mf} = i2\pi k_0 n_g \alpha \int d^2 r_\perp n^2 \mathbf{u}^{(\beta_0,m,f)*}(\mathbf{r}_\perp) \cdot \sum_{f',m'=\pm 1} \left[\mathbf{u}^{(\beta_0,m',f')}(\mathbf{r}_\perp) \mathbf{u}^{(\beta_0,m',f')*}(\mathbf{r}'_\perp) \right] \cdot \mathbf{u}^{(\beta_0,1,1)}(\mathbf{r}'_\perp)$$

$$e^{if'\beta_0(z-z')} e^{i\beta_0(z'-fz)} \tag{20}$$

$$= i2\pi k_0 n_g \alpha \mathbf{u}^{(\beta_0,m,f)*}(r'_\perp) \cdot \mathbf{u}^{(\beta_0,1,1)}(r'_\perp) e^{i\beta_0(1-f)z' + i(1-m)\phi'}, \tag{21}$$

where the orthogonality relationship of the fiber modes had been used:

$$\int n^2(\mathbf{r}) \mathbf{u}^{(\mu)}(\mathbf{r}) \cdot \mathbf{u}^{(\mu')*}(\mathbf{r}) d\mathbf{r}_\perp = \delta_{\mu\mu'} \tag{22}$$

$$\Leftrightarrow \int_0^{2\pi} d\phi \int_0^\infty r_\perp dr_\perp n^2(r_\perp) \mathbf{u}^{(\beta_0,m,f)}(r_\perp) \cdot \mathbf{u}^{(\beta_0,m',f')*}(r_\perp) e^{i(f-f')\beta_0 z + i(m-m')\phi} = \delta_{mm'} e^{i(f-f')\beta_0 z}. \tag{23}$$

The output forwarding $m = 1$ HE$_{11}$ mode component becomes

$$\mathbf{E}_+(\mathbf{r}) = (1 + C_{11}) E_0 \mathbf{u}_{(\beta_0,1,1)}(\mathbf{r}) \tag{24}$$

$$\approx \exp\left[i2\pi k_0 n_g \alpha |\mathbf{u}^{(\beta_0,1,1)}(r'_\perp)|^2 \right] E_0 \mathbf{u}^{(\beta_0,1,1)}(\mathbf{r}) \tag{25}$$

$$= t e^{i\delta\phi} E_{in}(\mathbf{r}), \tag{26}$$

where the attenuation factor of the mode is

$$t = \exp\left[\mathrm{Im}[C_{11}] \right] = \exp\left[-2\pi k_0 n_g \mathrm{Im}[\alpha] |\mathbf{u}^{(\beta_0,1,1)}(r'_\perp)|^2 \right] \tag{27}$$

and the phase shift is

$$\delta\phi = \mathrm{Re}[C_{11}] = 2\pi \mathrm{Re}[\alpha] \frac{\omega_0}{v_g} |\mathbf{u}^{(\beta_0,1,1)}(r'_\perp)|^2 = 2\pi \mathrm{Re}[\alpha] \frac{\omega_0}{cA_{11}^g}, \tag{28}$$

where $A_{mf}^g = 1/n_g |\mathbf{u}^{(\beta_0,m,f)}(r'_\perp)|^2$ is the effective $\mu = (\beta_0, m, f)$ mode area at the atom position.

We use the fact that

$$\alpha = -\frac{|d_{eg}|^2}{\hbar\Delta}, \quad (\Delta = \omega_0 - \omega_{eg}) \tag{29}$$

9

$$\Gamma_{mf}^g = 2\pi \frac{|\mathbf{u}^{(\mu)}(\mathbf{r}') \cdot \mathbf{d}_{eg}|^2}{\hbar} \left(\frac{\omega_0}{v_g}\right) \tag{30}$$

$$\Gamma = \frac{4}{3} \left(\frac{\omega_0}{c}\right)^3 \frac{|d_{eg}|^2}{\hbar} \tag{31}$$

$$\sigma_0 = \frac{3\lambda^2}{2\pi} \equiv \text{resonant cross section} \tag{32}$$

the phase shift can be rewritten as

$$\delta\phi = -\frac{\Gamma_{11}^g}{\Delta} = -\frac{\sigma_0}{A_{mf}^g} \frac{\Gamma}{4\Delta} = -n_g \sigma_0 |\mathbf{u}_1^1(r_\perp')|^2 \frac{\Gamma}{4\Delta}. \tag{33}$$

Notice that, the phase shift result is valid for scalar polarizability atoms, in which the induced dipole moment $\mathbf{d}_{eg} = \alpha \mathbf{u}^{(\mu)}(\mathbf{r}')$ along the same direction as the guided field, and hence $\Gamma_{mf}^g = 2\pi \frac{|\mathbf{d}_{eg}|^2}{\hbar A_{mf}^g} \left(\frac{\omega_0}{c}\right)$. For a more general case where the atomic polarizability can be a tensor, the phase shift can be given by

$$\delta\phi = 2\pi \frac{\omega_0}{v_g} \mathbf{u}^{(\beta_0,1,1)}(r_\perp') \cdot \text{Re}[\quad] \cdot \mathbf{u}^{(\beta_0,1,1)*}(r_\perp') = -2\pi \frac{\omega_0}{v_g} \frac{|\mathbf{u}^{(\mu)}(\mathbf{r}') \cdot \mathbf{d}_{eg}|^2}{\hbar \Delta} = -\frac{\Gamma_{11}^g}{\Delta}. \tag{34}$$

Therefore, Equ. 33 is valid for a general atomic polarizability.

If there are two input modes, the Faraday and birefringence effects can be analyzed along this line. A more generalized result for a two-side chain case is given in Section III C.

B. Connect to the Heisenberg picture

Need to decide if we should put the detailed derivations to the appendix.

We consider a single mode interact with an atom again, in which the Hamiltonian can be given by

$$\hat{H} = \hat{H}_0 + \hat{H}_{int}, \tag{35}$$

where the free field Hamiltonian can be given by

$$\hat{H}_0 = \sum_{m,f} \int \mathrm{d}\beta \hbar \omega_\beta \hat{a}_\mu^\dagger(\beta) \hat{a}_\mu(\beta) + \sum_{m,p} \int \mathrm{d}\beta \hbar \omega_\beta \hat{a}_\nu^\dagger(\beta) \hat{a}_\nu(\beta) + \hat{H}_A \tag{36}$$

$$= \sum_{m,f} f \int \mathrm{d}\omega \hbar \omega \hat{a}_\mu^\dagger(\omega) \hat{a}_\mu(\omega) + \sum_{m,p} \int \mathrm{d}\omega \hbar \omega \hat{a}_\nu^\dagger(\omega) \hat{a}_\nu(\omega) + \frac{\hbar \omega_{eg}}{2} \hat{\sigma}_z, \tag{37}$$

with $\hat{a}_\mu(\omega) = \sqrt{\left|\frac{\mathrm{d}\beta}{\mathrm{d}\omega}\right|} \hat{a}_\mu(\beta) = \frac{1}{\sqrt{v_g}} \hat{a}_\mu(\beta)$ and $\hat{a}_\nu(\omega) = \frac{1}{\sqrt{c}} \hat{a}_\nu(\beta)$. For the two-direction propagating guided modes, we have linearized the frequency as $\omega \approx \omega_0 + f v_g (\beta - f \beta_0)$. Just

for this section, we define $\mu = (\omega, f = \pm 1, m = \pm 1)$ to indicate the guided modes and $\nu = (\omega, \beta, m, p)$ for the radiative modes, where for the radiative modes $m = 0, \pm 1, \pm 2, \cdots$ are the mode orders and $p = \pm 1$ denote the two degrees of freedom of the mode polarizations. We consider the atomic Hamiltonian $\hat{H}_A = \frac{\hbar\omega_{eg}}{2}\hat{\sigma}_z$ to represent a two-level system. The interaction Hamiltonian is

$$\hat{H}_{int} = -\hat{\mathbf{d}} \cdot \hat{\mathbf{E}} = -\hat{\mathbf{d}}_{eg} \cdot \hat{\mathbf{E}}^{(+)}(\mathbf{r}') - \hat{\mathbf{d}}_{ge} \cdot \hat{\mathbf{E}}^{(-)}(\mathbf{r}'), \tag{38}$$

where the electric field operator $\hat{\mathbf{E}}^{(+)} = \hat{\mathbf{E}}_g^{(+)} + \hat{\mathbf{E}}_r^{(+)}$ with the guided mode and radiative mode contributions expressed respectively as

$$\hat{\mathbf{E}}_g^{(+)}(\mathbf{r}) = \sum_{m,f} \int d\omega \sqrt{\frac{\hbar\omega}{v_g}} \hat{a}_\mu(\omega) \mathbf{u}^{(\mu)}(\mathbf{r}_\perp) e^{if\beta z} \tag{39}$$

$$\hat{\mathbf{E}}_r^{(+)}(\mathbf{r}) = \sum_{m,p} \int d\omega \int_{-kn_2}^{kn_2} d\beta \sqrt{\hbar\omega} \hat{a}_\nu(\omega) \mathbf{u}^{(\nu)}(\mathbf{r}_\perp) e^{i\beta z}. \tag{40}$$

We define the coupling strength between the electric dipole and the guided electric field $\mathbf{u}^{(\mu)}(\mathbf{r}')$ or the radiative electric field $\mathbf{u}^{(\nu)}(\mathbf{r}')$ at the dipole position as

$$\hbar g_\mu(\omega) = \sqrt{\frac{\hbar\omega}{v_g}} \mathbf{d}_{eg} \cdot \mathbf{u}^{(\mu)}(\mathbf{r}') \tag{41}$$

$$\hbar g_\nu(\omega) = \int_{-kn_2}^{kn_2} d\beta \sqrt{\hbar\omega} \mathbf{d}_{eg} \cdot \mathbf{u}^{(\nu)}(\mathbf{r}'). \tag{42}$$

The atomic raising dipole operator $\hat{\mathbf{d}}_{eg} = \mathbf{d}_{eg}\hat{\sigma}_+ = \langle e|\mathbf{D}|g\rangle\hat{\sigma}_+$. Using the relationships defined above, the interaction Hamiltonian can then be simplified as

$$\hat{H}_{int} = -\sum_{m,f} \int d\omega \hbar \left[g_\mu(\omega)\hat{a}_\mu\hat{\sigma}_+ + g_\mu^*(\omega)\hat{a}_\mu^\dagger\hat{\sigma}_- \right] - \sum_{m,p} \int d\omega \hbar \left[g_\nu(\omega)\hat{a}_\nu\hat{\sigma}_+ + g_\nu^*(\omega)\hat{a}_\nu^\dagger\hat{\sigma}_- \right]. \tag{43}$$

Assuming all operators are not explicitly time-dependent, the Heisenberg equations of motion can then be rewritten as

$$\frac{d\hat{a}_\mu}{dt} = -if\omega\hat{a}_\mu + ig_\mu^*(\omega)\hat{\sigma}_- \tag{44}$$

$$\frac{d\hat{a}_\nu}{dt} = -i\omega\hat{a}_\nu + ig_\nu^*(\omega)\hat{\sigma}_- \tag{45}$$

$$\frac{d\hat{\sigma}_-}{dt} = -i\omega_{eg}\hat{\sigma}_- - i\int_0^\infty d\omega \left[\sum_{m,f} g_\mu(\omega)\hat{a}_\mu(\omega) + \sum_{m,p} g_\nu(\omega)\hat{a}_\nu(\omega) \right] \hat{\sigma}_z. \tag{46}$$

We have used the commutators that $[\hat{a}_\mu(\omega'), \hat{a}_\mu^\dagger(\omega)] = \delta(\omega' - \omega)$, $[\hat{a}_\mu(\omega), \hat{a}_\nu^\dagger(\omega)] = 0$, $[\hat{\sigma}_+, \hat{\sigma}_-] = \hat{\sigma}_z$ and $[\sigma_z, \sigma_\pm] = \pm 2\sigma_z$. By multiplying a factor of $e^{if\omega t}$ or $e^{i\omega t}$ and integrating from an initial time t_0 to t on the first two equations above respectively, one can obtain the formal solution that

$$\hat{a}_\mu(\omega, t) \equiv \hat{a}_\mu^{out}(\omega) = \hat{a}_\mu(\omega, t_0) e^{-if\omega(t-t_0)} + ig_\mu^*(\omega) \int_{t_0}^t dt' e^{-if\omega(t-t')} \hat{\sigma}_-(t') \qquad (47a)$$

$$\hat{a}_\nu(\omega, t) \equiv \hat{a}_\nu^{out}(\omega) = \hat{a}_\nu(\omega, t_0) e^{-i\omega(t-t_0)} + ig_\nu^*(\omega) \int_{t_0}^t dt' e^{-i\omega(t-t')} \hat{\sigma}_-(t'). \qquad (47b)$$

We substitute the formal solution above into Equ. (46), and rewrite

$$\frac{d\hat{\sigma}_-}{dt} = -i\omega_{eg}\hat{\sigma}_- + \int_{t_0}^t dt' \int_0^\infty d\omega \left[\sum_{m,f} |g_\mu(\omega)|^2 e^{-if\omega(t-t')} + \sum_{m,p} |g_\nu(\omega)|^2 e^{-i\omega(t-t')} \right] \hat{\sigma}_z(t)\hat{\sigma}_-(t')$$

$$- i \int_0^\infty d\omega \left[\sum_{m,f} g_\mu(\omega)\hat{a}_\mu(\omega, t_0) e^{-if\omega(t-t_0)} + \sum_{m,p} g_\nu(\omega)\hat{a}_\nu(\omega, t_0) e^{-i\omega(t-t_0)} \right] \hat{\sigma}_z(t). \quad (48)$$

In the Markoff approximation that $\int_0^\infty d\omega\, e^{-i\omega f(t-t')} |g_i(\omega)|^2 \hat{\sigma}_-(t') \approx \pi\delta(t-t')|g_i(\omega_{eg})|^2 \hat{\sigma}_-(t)$ with $i = \{\mu, \nu\}$, one can then obtain

$$\frac{d\hat{\sigma}_-}{dt} = -i\omega_{eg}\hat{\sigma}_- + \left[\sum_{m,f} \pi|g_\mu(\omega_{eg})|^2 + \sum_{m,p} \pi|g_\nu(\omega_{eg})|^2 \right] \hat{\sigma}_z(t)\hat{\sigma}_-(t)$$

$$- i \int_0^\infty d\omega \left[\sum_{m,f} g_\mu(\omega)\hat{a}_\mu(\omega, t_0) e^{-if\omega(t-t_0)} + \sum_{m,p} g_\nu(\omega)\hat{a}_\nu(\omega, t_0) e^{-i\omega(t-t_0)} \right] \hat{\sigma}_z(t) \quad (49)$$

$$= (-i\omega_{eg} - \frac{\Gamma}{2})\hat{\sigma}_-(t)$$

$$- i \int_0^\infty d\omega \left[\sum_{m,f} g_\mu(\omega)\hat{a}_\mu(\omega, t_0) e^{-if\omega(t-t_0)} + \sum_{m,p} g_\nu(\omega)\hat{a}_\nu(\omega, t_0) e^{-i\omega(t-t_0)} \right] \hat{\sigma}_z(t), \quad (50)$$

where we have used $\hat{\sigma}_z\hat{\sigma}_- = -\hat{\sigma}_-$. We also used the definitions as will be shown below for the total decay rate of an atom in presence of a nanofiber, Γ, a component of the *one dimensional* decay rate due to a guided mode, Γ_{mf}^g, the decay rate due to a radiative mode, Γ_ν^r, and the corresponding total decay rate for the guided modes and radiative modes, Γ^g and Γ^r, given by

$$\Gamma_{mf}^g = 2\pi|g_\mu(\omega_{eg})|^2 = \frac{2\pi|\mathbf{u}^{(\mu)}(\mathbf{r}') \cdot \mathbf{d}_{eg}|^2}{\hbar} \left(\frac{\omega_{eg}}{v_g}\right) \qquad (51)$$

$$\Gamma_\nu^r = 2\pi|g_\nu(\omega_{eg})|^2 = \int_{-kn_2}^{kn_2} d\beta \frac{2\pi|\mathbf{u}^{(\nu)}(\mathbf{r}') \cdot \mathbf{d}_{eg}|^2 \omega_{eg}}{\hbar} \qquad (52)$$

12

$$\Gamma^g = \sum_{m,f} \Gamma^g_{mf}, \qquad \Gamma^r = \sum_{m,p} \Gamma^r_{\nu} \tag{53}$$

$$\Gamma = \Gamma^g + \Gamma^r. \tag{54}$$

What we are interested in is the frequency response of the guided modes at a given ω. We can use the definitions of the Fourier transformation and the inverse given by

$$\hat{\sigma}_-(t) = \int_0^\infty \frac{\mathrm{d}\omega}{\sqrt{2\pi}} \hat{\sigma}_-(\omega) e^{-i\omega(t-t_0)} \tag{55}$$

$$\hat{\sigma}_-(\omega) = \int_{t_0}^\infty \frac{\mathrm{d}t}{\sqrt{2\pi}} \hat{\sigma}_-(t) e^{i\omega(t-t_0)}, \tag{56}$$

and considering the weak saturation case that $\hat{\sigma}_z \approx -1$ or almost all atoms are in the ground state. Now that Equ. (50) becomes

$$-i\omega\hat{\sigma}_-(\omega) = \left[-i\omega_{eg} - \frac{\Gamma}{2} \right] \hat{\sigma}_-(\omega)$$
$$+ i\sqrt{2\pi} \left[\sum_{m,f} g_\mu(\omega)\hat{a}^{in}_\mu(\omega) e^{i\omega(t-t_0)} + \sum_{m,p} g_\nu(\omega)\hat{a}^{in}_\nu(\omega) e^{i\omega(t-t_0)} \right], \tag{57}$$

where we have defined $\hat{a}^{in}_\mu(\omega) \equiv \hat{a}_\mu(\omega, t_0) e^{-if\omega(t-t_0)}$ and $\hat{a}^{in}_\nu(\omega) \equiv \hat{a}_\nu(\omega, t_0) e^{-i\omega(t-t_0)}$. Therefore, we can obtain the linear response relationship between $\hat{\sigma}_-(\omega)$ and $\hat{a}^{in}(\omega)$ as

$$\hat{\sigma}_-(\omega) = -\sum_{m,f} \frac{\sqrt{2\pi} g_\mu(\omega) e^{i\omega(t-t_0)}}{\Delta + i\frac{\Gamma}{2}} \hat{a}^{in}_\mu(\omega) - \sum_{m,p} \frac{\sqrt{2\pi} g_\nu(\omega) e^{i\omega(t-t_0)}}{\Delta + i\frac{\Gamma}{2}} \hat{a}^{in}_\nu(\omega), \tag{58}$$

where the detuning $\Delta = \omega - \omega_{eg}$. The factor of $e^{i\omega(t-t_0)}$ is the accumulated phase factor due to the free evolution of light from time t_0 to t?

On the other hand, Equ. (47) implies the input-output relationship in the frequency domain $(t \gg t_0)$ that

$$\hat{a}^{out}_\mu(\omega) = \hat{a}^{in}_\mu(\omega) + i\sqrt{2\pi} g^*_\mu(\omega) \hat{\sigma}_-(\omega). \tag{59}$$

By substituting Equ. (58) into the equation above, we obtain the input-output relationships of the guided modes due to the presence of an atom close to the nanofiber as

$$\hat{a}^{out}_\mu(\omega) = \hat{a}^{in}_\mu(\omega) - i\sum_{m',f'} \frac{2\pi g^*_\mu(\omega) g_{\mu'}(\omega) e^{i\omega(t-t_0)}}{\Delta + i\frac{\Gamma}{2}} \hat{a}^{in}_{\mu'}(\omega) - i\sum_{m,p} \frac{2\pi g^*_\mu(\omega) g_\nu(\omega) e^{i\omega(t-t_0)}}{\Delta + i\frac{\Gamma}{2}} \hat{a}^{in}_\nu(\omega) \tag{60}$$

$$\approx \hat{a}^{in}_\mu(\omega) - i\sum_{m',f'} \frac{2\pi g^*_\mu(\omega) g_{\mu'}(\omega) e^{i\omega(t-t_0)}}{\Delta + i\frac{\Gamma}{2}} \hat{a}^{in}_{\mu'}(\omega) = \sum_{\mu'} S^\mu_{\mu'} \hat{a}^{in}_{\mu'}(\omega), \tag{61}$$

13

where the S matrix elements

$$S^{\mu}_{\mu'} \equiv S^{mf}_{m'f'} = \delta_{mm'}\delta_{ff'} - i\frac{2\pi g^*_{\mu}(\omega)g_{\mu'}(\omega)e^{i\omega(t-t_0)}}{\Delta + i\frac{\overline{\cdot}}{2}}, \tag{62}$$

and we have ignored the crossing terms between the guided modes and radiative modes due to orthogonality.

For the $m = 1, f = 1$ mode, for instance, if we ignore the portions scattered to all the other modes and the time-dependent phase factor, we will have

$$\hat{a}^{out}_{\mu}(\omega) \approx \left[1 - i\frac{\Gamma^g_{mf}}{\Delta + i\Gamma/2}\right]\hat{a}^{in}_{\mu}(\omega) \tag{63}$$

$$= \left(\frac{\Delta + i(\Gamma/2 - \Gamma^g_{mf})}{\Delta + i\frac{\overline{\cdot}}{2}}\right)\hat{a}^{in}_{\mu}(\omega). \tag{64}$$

In absence of scattering, the transmitted guided mode has a phase shift effect that the transmission coefficient is

$$t(\omega) = e^{i\delta\phi(\omega)}, \tag{65}$$

where the phase shift in the dispersive regime $(\Delta \gg \Gamma^g_{mf})$ is

$$\delta\phi \approx -\tan^{-1}\left(\frac{\Gamma^g_{mf}}{\Delta}\right) \approx -\frac{\Gamma^g_{mf}}{\Delta} = -2\pi\frac{|d_{eg}|^2}{\hbar\Delta}\frac{\omega}{cA^g_{mf}} = 2\pi\frac{\alpha}{A^g_{mf}}\frac{\omega}{c}. \tag{66}$$

> Need to be more careful about the $e^{i\omega(t-t_0)}$ phase factor and its physics interpretation...

To generalize our results to a real atom case, we need to replace the two-level dipole operator with

$$\hat{\mathbf{d}}^{\dagger}_{f'f} = \sum_{q}\sum_{m,m'}\langle f'm'|d^q_{f',f}|fm\rangle|f'm'\rangle\langle fm|\mathbf{e}^*_q \tag{67}$$

$$= \langle f'||d||f\rangle\sum_{q}\sum_{m,m'}\langle fm; 1q \,|\, f'm'\rangle|f'm'\rangle\langle fm|\mathbf{e}^*_q, \tag{68}$$

which raises the atom from the ground hyperfine state f to the excited state f'. Correspondingly, the raising operator should be defined as

$$\hat{\sigma}^{f'm'fm}_+ = |f'm'\rangle\langle fm|. \tag{69}$$

Therefore, to generalize the input-output formalism derived above to the real atom case, we need to sum over all relevant ground states and excited states in terms of hyperfine sublevels.

14

C. Enhancement compared to the vacuum case

Notice that, the phase shift for an atom in vacuum can be given in a similar form by

$$\delta\phi^{vac} = 2\pi\frac{\omega_0}{cA}\Re[\alpha]|\mathbf{u}_{00}(\mathbf{r}')|^2 = 2\pi\frac{\omega_0}{cA_{eff}^{vac'}}\Re[\alpha] = -\frac{1}{A}\sigma_0|\mathbf{u}_{00}(r_\perp')|^2\frac{\Gamma_{vac}}{4\Delta} = \frac{\Gamma_{1D}}{\Delta}, \qquad (70)$$

where $\mathbf{u}_{00}(\mathbf{r}')$ is the TEM$_{00}$ mode of a Gaussian laser field at the atom position, $A = \frac{\pi W_0^2}{2}$ is the mode area of the Gaussian beam with wist W_0, and $\Gamma_{1D} = 2\pi\frac{|d_{eg}|^2|\mathbf{u}_{00}(\mathbf{r}')|^2}{\hbar A}\left(\frac{\omega_0}{c}\right)$. We can define the effective mode area $A_{eff}^{vac'} = \frac{A}{|\mathbf{u}_{00}(\mathbf{r}')|^2}$, and then everything here is comparable to the fiber case. Hence, the relative strength of phase shift due to the presence of a nanofiber versus vacuum can be given by

$$\frac{\delta\phi^{nano}}{\delta\phi^{vac}} = \frac{A_{eff}^{vac'}}{A_{11}^g} = An_g\frac{|\mathbf{u}^{(\beta_0,1,1)}(r_\perp^{nano'})|^2}{|\mathbf{u}_{00}(r_\perp^{vac'})|^2}. \qquad (71)$$

In the vacuum case, the strongest mode is given by $|\mathbf{u}_{00}(r_\perp^{vac'})| = 1$ when the atom is placed at the symmetry center of the beam waist.

Figure for the enhancement comparison.
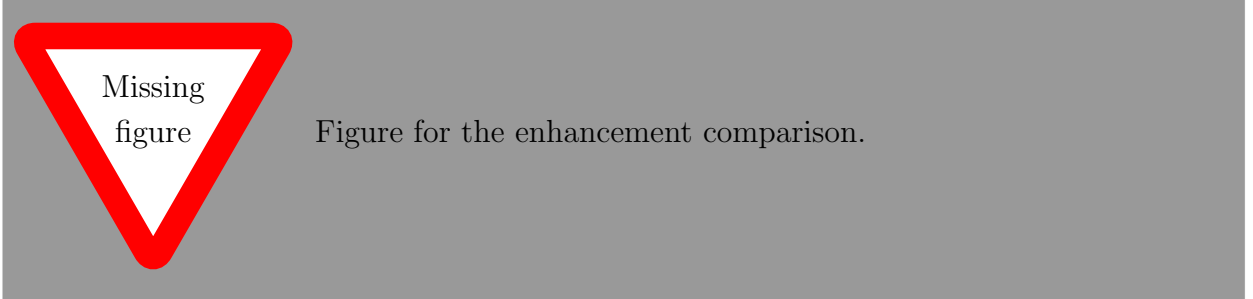
D. Quantum interface for the nano ber with clock state

Need to decide if we should put the detailed derivations to the appendix.

We present a general theory on light-atom interaction in presence of a nanofiber in Appendix C. Here, we consider a simple case that all trapped cesium atoms are initially pumped and restricted to the clock states of the ground state $(6S_{1/2})$ sublevels, in which the atomic magnetic quantum number $M = 0$ while the total atomic angular momentum quantum number can be $F = 3$ and $F = 4$. Therefore, we only care about the atomic polarizability components

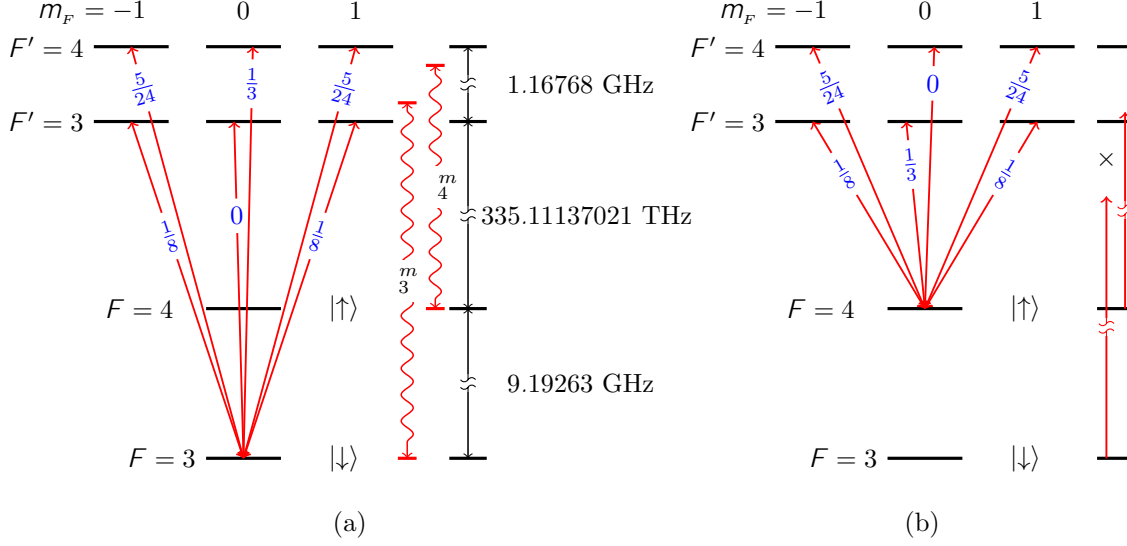$$\uparrow = \langle F = 4, M = 0| \ |F = 4, M = 0\rangle \qquad (72)$$

FIG. 2: Hyperfine level structure of the D_1 line transitions involving the clock states in $6S_{1/2}$ ground levels, their transition probabilities (numbers on the straight transition lines) and the two magic wavelength positions (wiggled lines). Subfig. 2a shows the transitions only involving the $F = 3, m = 0$ manifold. Subfig. 2b shows the transitions only involving the $F = 4, m = 0$ manifold.

$$\downarrow = \langle F = 3, M = 0| \quad |F = 3, M = 0\rangle. \tag{73}$$

Suppose there are H and V two orthogonal linear polarized mode components. The quantized forward-propagating electric field can be given by

$$\hat{\mathbf{E}}^{(+)}(r_\perp, \phi, z) = \sqrt{\frac{2\pi\hbar\omega_0}{v_g\tau}}\left(\mathbf{u}_H(r_\perp, \phi)\hat{a}_H + \mathbf{u}_V(r_\perp, \phi)\hat{a}_V\right)e^{i\beta_0 z}. \tag{74}$$

The Hamiltonian due to the light-atom interaction can be written as

$$H_{\mathrm{e}} = -\hat{\mathbf{E}}^{(-)}(r_\perp', \phi', z') \cdot \quad \cdot \hat{\mathbf{E}}^{(+)}(r_\perp', \phi', z') \tag{75}$$

$$= -\sum_{F,F'}\alpha_0(\Delta_{F,F'})\left\{C^{(0)}_{J'FF}\hat{\mathbf{E}}^{(-)} \cdot \hat{\mathbf{E}}^{(+)}\hat{\mathbb{1}}_F\right.$$

$$+ iC^{(1)}_{J'FF'}\left(\hat{\mathbf{E}}^{(-)} \times \hat{\mathbf{E}}^{(+)}\right) \cdot \hat{\mathbf{F}}$$

$$\left.+ C^{(2)}_{J'FF}\hat{E}^{(-)}_i\hat{E}^{(+)}_j\left(\frac{\hat{F}_i\hat{F}_j + \hat{F}_j\hat{F}_i}{2} - \frac{1}{3}\delta_{ij}\hat{\mathbf{F}} \cdot \hat{\mathbf{F}}\right)\right\}. \tag{76}$$

Note: the effective Hamiltonian expressed in terms of Clebsch-Gordan coefficients in stead of the reduced coefficients is given in Appendix D.

16

In the equation above, we have defined J as the total electric angular momentum quantum number, and the characteristic polarizability of the atom can be given by

$$\alpha_0(\Delta) = -\frac{|\langle J'||d||J\rangle|^2}{\hbar\Delta} = -\frac{3\lambda_{J'J}^3}{32\pi^3}\frac{\Gamma}{\Delta} \quad \text{with} \quad \Gamma = \frac{1}{\hbar}\frac{4}{3}\frac{\omega_{JJ'}^3}{c^3}|\langle J'||d||J\rangle|^2. \tag{77}$$

In our case, the vector component of the atomic polarizability is zero. We can ignore the tensor component of the atomic polarizability in the far off-resonance regime. The scalar polarizability coefficient can be specified for our case as

$$C_{J'F}^{(0)} \equiv \sum_{F'} C_{J'FF'}^{(0)} = \frac{2^{J'-1/2}}{3} = \left\{\frac{1}{3}, \frac{2}{3}\right\}. \tag{78}$$

The two values in the brackets are for the D_1 and D_2 lines, respectively.

The Hamiltonian can be further rewritten as

$$\begin{aligned}
H_e &= \frac{\hbar}{\tau}\left(\chi_{H,\uparrow}|\uparrow\rangle\langle\uparrow| + \chi_{H,\downarrow}|\downarrow\rangle\langle\downarrow|\right)\hat{a}_H^\dagger\hat{a}_H \\
&+ \frac{\hbar}{\tau}\left(\chi_{V,\uparrow}|\uparrow\rangle\langle\uparrow| + \chi_{V,\downarrow}|\downarrow\rangle\langle\downarrow|\right)\hat{a}_V^\dagger\hat{a}_V,
\end{aligned} \tag{79}$$

where the coupling strengths are defined as

$$\chi_{H,\uparrow} = -\frac{2\pi\omega_0}{v_g}\mathbf{u}_H^*(r_\perp', \phi') \cdot \overleftrightarrow{\alpha}_\uparrow \cdot \mathbf{u}_H(r_\perp', \phi') \tag{80}$$

$$\chi_{H,\downarrow} = -\frac{2\pi\omega_0}{v_g}\mathbf{u}_H^*(r_\perp', \phi') \cdot \overleftrightarrow{\alpha}_\downarrow \cdot \mathbf{u}_H(r_\perp', \phi') \tag{81}$$

$$\chi_{V,\uparrow} = -\frac{2\pi\omega_0}{v_g}\mathbf{u}_V^*(r_\perp', \phi') \cdot \overleftrightarrow{\alpha}_\uparrow \cdot \mathbf{u}_V(r_\perp', \phi') \tag{82}$$

$$\chi_{V,\downarrow} = -\frac{2\pi\omega_0}{v_g}\mathbf{u}_V^*(r_\perp', \phi') \cdot \overleftrightarrow{\alpha}_\downarrow \cdot \mathbf{u}_V(r_\perp', \phi'). \tag{83}$$

with $\overleftrightarrow{\alpha}_\uparrow \approx \sum_{F'=3,4}\frac{\alpha_0(\Delta_{4,F'})}{3}\mathbf{I}$ and $\overleftrightarrow{\alpha}_\downarrow \approx \sum_{F'=3,4}\frac{\alpha_0(\Delta_{3,F'})}{3}\mathbf{I}$. One can use different detuning regimes to detect the atomic clock state as a psuedo-spin state.

The coupling strength for the D_1 line probing can then be written as

$$\chi_{H,\uparrow} = \sum_{F'}\frac{\chi_{H0}(F', 4)}{3}, \qquad\qquad \chi_{H,\downarrow} = \sum_{F'}\frac{\chi_{H0}(F', 3)}{3}, \tag{84}$$

$$\chi_{V,\uparrow} = \sum_{F'}\frac{\chi_{V0}(F', 4)}{3}, \qquad\qquad \chi_{V,\downarrow} = \sum_{F'}\frac{\chi_{V0}(F', 3)}{3} \tag{85}$$

and

$$\chi_{H0}(F', F) = \left(\frac{\sigma_0}{A_{eff}^H}\right)\left(\frac{\Gamma}{4\Delta_{F,F'}}\right) = \frac{\Gamma_H^{1D}}{\Delta_{F,F'}}, \qquad\qquad A_{eff}^H = \frac{1}{n_g|\mathbf{u}_H(r_\perp', \phi')|^2}, \tag{86}$$
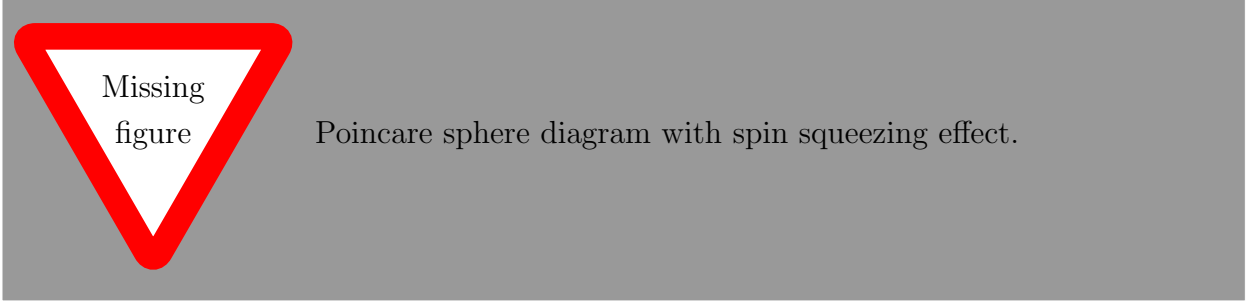
$$\chi_{V0}(F', F) = \left(\frac{\sigma_0}{A_{eff}^V}\right)\left(\frac{\Gamma}{4\Delta_{F,F'}}\right) = \frac{\Gamma_V^{1D}}{\Delta_{F,F'}}, \qquad A_{eff}^V = \frac{1}{n_g|\mathbf{u}_V^*(r'_\perp, \phi')|^2}. \qquad (87)$$

The Hamiltonian can also be rewritten as below using the Stokes operators, $\hat{S}_q$, and collective spin operators, $\hat{J}_q$, with $q = 0, 1, 2, 3$.

$$\begin{aligned}
H_e &= \frac{\hbar}{\tau}\Big\{ \left[(\chi_{H,\uparrow} + \chi_{H,\downarrow}) + (\chi_{V,\uparrow} + \chi_{V,\downarrow})\right]\hat{J}_0\hat{S}_0 \\
&\quad + \left[(\chi_{H,\uparrow} + \chi_{H,\downarrow}) - (\chi_{V,\uparrow} + \chi_{V,\downarrow})\right]\hat{J}_0\hat{S}_1 \\
&\quad + \left[(\chi_{H,\uparrow} - \chi_{H,\downarrow}) + (\chi_{V,\uparrow} - \chi_{V,\downarrow})\right]\hat{J}_3\hat{S}_0 \\
&\quad + \left[(\chi_{H,\uparrow} - \chi_{H,\downarrow}) - (\chi_{V,\uparrow} - \chi_{V,\downarrow})\right]\hat{J}_3\hat{S}_1 \Big\}.
\end{aligned} \qquad (88)$$

Poincare sphere diagram with spin squeezing effect.

The first term is an overall scalar shift and thus does not contribute to the relative dynamics. The second term is a constant birefringence and can be canceled with a compensating waveplate as long as the atom number remains constant which is usually the case when the trapping time is fairly large compared to the measurement time. The first two terms can also be canceled when we have the detuning approximately equally biased for the $F = 3$ and $F = 4$ ground states. For example, we can choose $\Delta_3 = -4.6$ GHz and $\Delta_4 = 4.6$ GHz to the $6P_{1/2}$ excited state sublevels of cesium atoms to satisfy this condition, where the hyperfine splitting of the excited state can be ignored (500 MHz) compared to the detuning. However, we would like to leave the choice of detuning to control the third and fourth terms as will be discussed consequently.

The final term describes the QND Faraday interaction we wish to isolate (similar to the Faraday interaction since we choose to use the y-axis as the quantization axis), but this requires dealing with the third term that describes the effect of the scalar light shift on the rotation of the pseudo-spin. Canceling the third term amounts to enforcing the condition that

$$\chi_{H,\uparrow} - \chi_{H,\downarrow} = \chi_{V,\downarrow} - \chi_{V,\uparrow}, \qquad (89)$$

which can be satisfied if we carefully choose the detuning of the probe light. The wavelength to choose to cancel the third term is atom position related, since the condition is determined by the effective mode areas which may have different ratios for the H and V modes at different locations. We can refer the exact wavelength to satisfy this condition as the *magic wavelength*. If this condition can be met, then we can achieve an interaction of the form,

$$H_{\mathrm{e}} = \frac{\hbar}{\tau}\chi_{\mathrm{e}} \; \hat{J}_3 \hat{S}_1 \tag{90}$$

where $\chi_{\mathrm{e}} = 2(\chi_{H,\uparrow} - \chi_{H,\downarrow})$.

Using this, we can prepare the spins in D state on the Bloch sphere and characterize the collective spin state along the z-axis after the rotation along S_1 axis due to the photon-atom interaction. To achieve this, we use the $\hat{S}_3$ Stokes vector component measurement. As a result of the backaction of the polarization measurement, there is a squeezing to the collective spin state which results in a reduced uncertainty of measurement output. To see this, we assume the photon number, N_L, is large and apply the Holstein-Primakoff approximation to set $\hat{S}_1 = \sqrt{\frac{N_L}{2}}\hat{P}_L$ and $\hat{S}_3 = \sqrt{\frac{N_L}{2}}\hat{X}_L$, where $\hat{X}_L$ and $\hat{P}_L$ are two photonic quadratures satisfying the commutation relationship that $[\hat{X}_L, \hat{P}_L] = i$. Now the effective Hamiltonian can be written as

$$H_{\mathrm{e}} = \frac{\hbar}{\tau}\chi_{\mathrm{e}} \; \sqrt{\frac{N_L}{2}}\hat{J}_3 \hat{P}_L. \tag{91}$$

The $\hat{S}_3$ measurement is achieved through sending the signal light to one input port of a beam splitter along with a vacuum input on the other input port and then performing a balanced Homodyne measurement of the X_L quadrature. The equivalent Kraus operator conditional on this measurement can be defined by

$$\hat{A}_{X_L} = \langle X_L | e^{-i\chi_{\mathrm{eff}}\sqrt{\frac{N_L}{2}}\hat{J}_3\hat{P}_L}|0_L\rangle \propto \exp\left\{-\frac{\kappa T}{4}(l - \hat{J}_3)^2\right\}, \tag{92}$$

where $l = \frac{X_L}{\chi_{\mathrm{eff}}\sqrt{N_L/2}}$ is the measurement outcome in angular momentum units, and $\kappa T = \chi_{\mathrm{e}}^2 N_L$ is the integrated measurement strength per spin. The shot noise resolution of the QND measurement is $\sigma^2 = \frac{1}{\kappa T}$. The Kraus operator $\hat{A}_{X_L}$ yields a backaction and generates a spin squeezing state[Reference]. Given a spin coherent state (SCS) input with total spin quantum number $J = N_A/2$, the output state probability distribution can be given by

$$P_{L|l} \propto e^{-\frac{(L-\bar{L}(l))^2}{2\Delta J_{out}^2}}, \tag{93}$$

where $\Delta J^2_{out} = \frac{J^2_{in}}{1+\xi} = \frac{J}{2(1+\xi)}$, $\bar{L}(l) = \frac{l}{1+\xi}$, and $\xi \equiv \frac{J^2_{in}}{\sigma^2} = \frac{J}{2\sigma^2} = \frac{\chi^2_{eff}}{4} N_A N_L$ is the measurement strength which characterizes the measurement backaction and the squeezing effect. The ability to resolve the initial quantum variance of J_3 within the resolution of the meter is the key to QND squeezing.

E. Birefringence and Faraday spectroscopies

Discuss the homodyne detection and sensitivity to the atom number and operating frequency in the shot noise limit. It relates to (i) the phase shift and (ii) the shot noise resolution of the polarimeter. Should cover expectation value and fluctuation measurements.

For the birefringence measurement of the clock states discussed above, the fluctuation of the S_3 measurement is a combined effect of the shot noise fluctuation of the photon detector and the projection noise as the signal to determine the collective spin state. The square variance of the measurement is

$$\Delta L^2 = \Delta P^2_{SN} + \Delta P^2_S, \tag{94}$$

where ΔP^2_{SN} and ΔP^2_S are the square variances of the shot noise and the signal, respectively. The smallest detectable spin polarization change from the input state is determined by the shot noise limit condition that

$$\Delta P_S = \Delta P_{SN}, \tag{95}$$

where the standard variance of the signal can be estimated by

$$\Delta P_S = P_0 \sin(\varphi_N) \approx P_0 \varphi_N \tag{96}$$

and the shot noise variance is determined by [43]

$$\Delta P_{SN} = \sqrt{\frac{P_0 \hbar \omega_0}{2\eta \tau_{pd}}}. \tag{97}$$

Above, we have defined P_0 as the power of the input laser field, φ_N as the angle change of the output light on the Poincare sphere due to N_A atoms, η as the quantum efficiency of the photon detector, and τ_{pd} as the time constant of the detector.

Using the magic wavelengths, we have

$$\chi_e(\omega) = 2(\chi_{H,\uparrow} - \chi_{H,\downarrow}) \tag{98}$$

20

$$= 2\sigma_0 n_g \sum_q |\mathbf{e}_q \cdot \mathbf{u}_H^*(r'_\perp, \phi')|^2 \sum_{F'} \frac{\Gamma}{4} \left(\frac{|o_{J4}^{J'F'} C_{F'q}^{40;1q}|^2}{\Delta_{4F'} + i\Gamma/2} - \frac{|o_{J3}^{J'F'} C_{F'q}^{30;1q}|^2}{\Delta_{3F'} + i\Gamma/2} \right), \tag{99}$$

or, in the dyadic Green function language from Equ. D27,

$$\chi_e\ (\omega) = 8\pi k_0^2 \, \mathrm{tr} \left\{ \mathrm{Im} \left[\mathbf{G}_{HH}^*(\mathbf{r}'_\perp, \mathbf{r}'_\perp) \right] \cdot \left({}^{40;40} - {}^{30;30} \right) \right\}. \tag{100}$$

For the D_1 line transition, for example, there are two magic frequencies at ω_3^m and ω_4^m which close to the $F = 3 \leftrightarrow F' = 3$ and $F = 4 \leftrightarrow F' = 4$ transitions, respectively. In general, if we use the magic frequency, $\omega_F^{\mathrm{magic}}$, which close to the $F \leftrightarrow F' = F$ transition, we would have

$$\chi_e\ (\omega_F^m) = 8\pi k_0^2 \, \mathrm{tr} \left\{ \mathrm{Im} \left[\mathbf{G}_{HH}^*(\mathbf{r}'_\perp, \mathbf{r}'_\perp) \right] \cdot \left({}^{40;40}(\omega_F^m) - {}^{30;30}(\omega_F^m) \right) \right\} \tag{101}$$

$$= \sigma_0 n_g \frac{\Gamma}{2} \sum_q |\mathbf{e}_q \cdot \mathbf{u}_H^*(r'_\perp, \phi')|^2 \sum_{F'} \left(\frac{|o_{J4}^{J'F'} C_{F'q}^{40;1q}|^2}{\Delta_{4F'} + i\Gamma/2} - \frac{|o_{J3}^{J'F'} C_{F'q}^{30;1q}|^2}{\Delta_{3F'} + i\Gamma/2} \right), \tag{102}$$

The angle change on the Poincare sphere using the probe light at the magic frequency ω_F^m can be given by

$$\varphi_N(\omega_F^m) = N_A |\chi_{eff}(\omega_F^m)| \tag{103}$$

$$= N_A \sigma_0 n_g \frac{\Gamma}{2} \sum_q |\mathbf{e}_q \cdot \mathbf{u}_H^*(r'_\perp, \phi')|^2 \sum_{F'} \left(\frac{|o_{J3}^{J'F'} C_{F'q}^{30;1q}|^2}{\Delta_{3F'}} - \frac{|o_{J4}^{J'F'} C_{F'q}^{40;1q}|^2}{\Delta_{4F'}} \right). \tag{104}$$

We have ignored the decay rate whenever it is summed with the detuning terms.

Now, we consider the critical case that $\eta = 100\%$ and $\tau_{pd} = \frac{1}{\gamma_s}$, where the photon scattering rate

$$\gamma_s = \gamma_s(\omega_F) = \sum_{F,F'} \sigma(\Delta_{FF'}) \frac{I(\mathbf{r}')}{\hbar \omega_0}, \tag{105}$$

where I is the intensity of the light, and the photon scattering cross-section

$$\sigma(\Delta_{FF'}) = \frac{\sigma_0}{1 + \frac{4\ {}_{FF'}^2}{2}} = \frac{\sigma_0 \Gamma^2}{\Gamma^2 + 4\Delta_{FF'}^2} \approx \sigma_0 \frac{\Gamma^2}{4\Delta_{FF'}^2} \quad \text{(far detuning.)} \tag{106}$$

Hence, by using the relationships given above, we can rewrite

$$\Delta P_{SN}(\omega_F^m) = \frac{P_0 \Gamma}{2} \sqrt{\frac{\sigma_0}{2A_{in}} \sum_{F'} \left(\frac{1}{\Delta_{3F'}^2} + \frac{1}{\Delta_{4F'}^2} \right)}, \tag{107}$$

$$\Delta P_S(\omega_F^m) = P_0 \varphi_N(\omega_F^m)$$

$$\approx P_0 N_A \sigma_0 n_g \frac{\Gamma}{2} \sum_q |\mathbf{e}_q \cdot \mathbf{u}_H^*(r'_\perp, \phi')|^2 \sum_{F'} \left(\frac{|o_{J3}^{J'F'} C_{F'q}^{30;1q}|^2}{\Delta_{3F'}} - \frac{|o_{J4}^{J'F'} C_{F'q}^{40;1q}|^2}{\Delta_{4F'}} \right) \tag{108}$$

$$(109)$$

with the effective mode areas

$$A_{in} = \frac{P_0}{I(\mathbf{r}')} = \frac{2}{|\mathbf{u}_H(r'_\perp)|^2 + |\mathbf{u}_V(r'_\perp)|^2}. \tag{110}$$

Therefore, the minimum detectable atom number, N_A^{min}, can be obtained by forcing $\Delta P_s = \Delta P_{SN}$ as

$$N_A^{min}(\omega_F^m) = \sqrt{\frac{A_e^2}{2A_{in}\sigma_0}} \tag{111}$$

with the effective mode area defined as

$$A_e = \frac{\sqrt{\sum_{F'}\left(\frac{1}{\frac{2}{3F'}} + \frac{1}{\frac{2}{4F'}}\right)}}{n_g \sum_q |\mathbf{e}_q \cdot \mathbf{u}_H^*(r'_\perp, \phi')|^2 \sum_{F'}\left(\frac{|o_{J3}^{J'F'}C_{F'q}^{30;1q}|^2}{3F'} - \frac{|o_{J4}^{J'F'}C_{F'q}^{40;1q}|^2}{4F'}\right)}. \tag{112}$$

Aside—only considering the scalar polarizability effect: If we choose a detuning far-off the transition lines due to the hyperfine splitting of the excited states and ignore the tensor effect of the atomic polarizability, we will recover the simplified result given by Dawkins and coworkers [14]. The prove follows. Since the vector atomic polarizability vanish for the clock states, ignoring the tensor atomic polarizability means there is only scalar atomic polarizability left. Therefore, the effective coupling strength can be given by

$$\chi_{eff} = [(\chi_{H,\uparrow} - \chi_{H,\downarrow}) - (\chi_{V,\uparrow} - \chi_{V,\downarrow})] \tag{113}$$

$$= 2C_{J'}^{(0)}(\Gamma_H^{1D} - \Gamma_V^{1D})\frac{1}{\Delta} = \frac{C_{J'}^{(0)}\sigma_0\Gamma}{2}\left(\frac{1}{A_{eff}^H} - \frac{1}{A_{eff}^V}\right)\frac{1}{\Delta}, \tag{114}$$

and the angle change by

$$\varphi_N = N_A\chi_{eff} \tag{115}$$

$$= N_A C_{J'}^{(0)} n_g \sigma_0 \frac{\Gamma}{2\Delta}\left[|\mathbf{u}_H(r'_\perp)|^2 - |\mathbf{u}_V(r'_\perp)|^2\right], \tag{116}$$

where $\frac{1}{\cdot} = \frac{1}{2}\sum_{F'}(\frac{1}{F',4} - \frac{1}{F',3}) \approx \frac{1}{F',4}$ and $\sigma_0 = 3\lambda^2/2\pi$ is the resonant photon scattering cross-section of the atoms.

Now, we consider the critical case that $\eta = 100\%$ and $\tau_{pd} = \frac{1}{\gamma_s}$, where the photon scattering rate

$$\gamma_s = \sigma(\Delta)\frac{I(\mathbf{r}')}{\hbar\omega_0}, \tag{117}$$

where I is the intensity of the light, and the photon scattering cross-section

$$\sigma(\Delta) = \frac{\sigma_0}{1 + \frac{4\Delta^2}{\Gamma^2}} \approx \sigma_0 \frac{\Gamma^2}{4\Delta^2} \quad \text{(far detuning.)} \tag{118}$$

Hence, we can rewrite

$$\Delta P_{SN} = P_0 \sqrt{\frac{\sigma_0}{2A_{in}}} \frac{\Gamma}{2\Delta}, \tag{119}$$

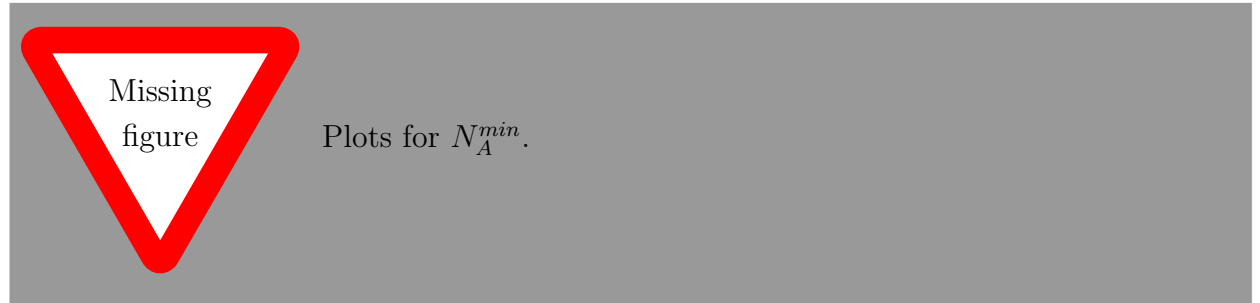$$\Delta P_S = N_A C_{j'}^{(0)} P_0 \frac{\sigma_0}{A_{eff}} \frac{\Gamma}{2\Delta}, \tag{120}$$

with the effective mode areas

$$A_{in} = \frac{P_0}{I(\mathbf{r}')} = \frac{2}{|\mathbf{u}_H(r_\perp')|^2 + |\mathbf{u}_V(r_\perp')|^2}, \tag{121}$$

$$A_{eff} = \frac{1}{n_g \left[|\mathbf{u}_H(r_\perp')|^2 - |\mathbf{u}_V(r_\perp')|^2 \right]}. \tag{122}$$

Therefore, the $\Delta P_S = \Delta P_{SN}$ condition gives the resolution of the birefringence measurement in terms of the minimum atom number as

$$N_A^{min} = \frac{1}{C_{J'}^{(0)}} \sqrt{\frac{A_{eff}^2}{A_{in} \sigma_0}}. \tag{123}$$

Missing
figure   Plots for N_A^{min}.

F.   Other applications?

III.   DISCUSSIONS

A.   Connect to the Schrodinger picture?

This has been done by Ben in one of his recent notes.

B. Achievable phase shift with scalar atomic polarizabilities?

To be deleted for this paper.

Show the phase shift and the decay rate are results of the combination effect of the free dipole radiation and the reflection from the nanofiber interface. Discuss the phase shift control landscape and the difference with the vacuum case. Apply to a phase gate.

$$\delta\phi = -\frac{\Gamma_\mu^{1D}}{2\Delta}, \tag{124}$$

$$\frac{\Gamma_\mu^{1D}}{\Gamma_0} = \frac{6\pi c}{\omega} \frac{\sum_g \mathbf{d}_{eg} \cdot \mathrm{Im}\left[\mathbf{G}_g^\mu(\mathbf{r}',\mathbf{r}')\right] \cdot \mathbf{d}_{eg}^*}{\sum_g |\mathbf{d}_{eg}|^2} = 1 + \frac{3}{2}\frac{\mathrm{Im}\left[\sum_g \mathbf{d}_{eg}^* \cdot \mathbf{E}_g^{(R,\mu)}(\mathbf{r}')\right]}{\sum_g |\mathbf{d}_{eg}|^2 k^3}$$

$$= \frac{3\pi}{2}\left(\frac{c}{\omega}\right)^2 \frac{c}{v_g} \frac{\sum_g |\mathbf{d}_{eg} \cdot \mathbf{u}^\mu(\mathbf{r}')|^2}{\sum_g |\mathbf{d}_{eg}|^2} \tag{125}$$

$$\mathbf{E}_g^{(R,\mu)}(\mathbf{r}') = -\frac{1}{4\pi k^2}\mathbf{G}_g^{(R,\mu)}(\mathbf{r}',\mathbf{r}') \cdot \mathbf{d}_{eg}. \tag{126}$$

The index R indicates the component of reflection, and $\mu = (\beta, m, f)$ identifies the normalized fiber mode $\mathbf{u}^\mu(\mathbf{r}')$.

We can write

$$\Gamma_{vac} = \frac{4\omega_0^3|\mathbf{d}|^2}{3\hbar c^3} = -\frac{8\pi\omega_0^2}{\hbar c^2}\left[\mathbf{d}\cdot\mathrm{Im}[\mathbf{G}^{(0)}(\mathbf{r}',\mathbf{r}')]\cdot\mathbf{d}^*\right] \tag{127}$$

$$\Gamma = -\frac{8\pi\omega_0^2}{\hbar c^2}\left[\mathbf{d}\cdot\mathrm{Im}[\mathbf{G}(\mathbf{r}',\mathbf{r}')]\cdot\mathbf{d}^*\right] = -\frac{8\pi\omega_0^2}{\hbar c^2}\left[\mathbf{d}\cdot\mathrm{Im}[\mathbf{G}^{(0)}(\mathbf{r}',\mathbf{r}') + \mathbf{G}^{(R)}(\mathbf{r}'\mathbf{r}')]\cdot\mathbf{d}^*\right] \tag{128}$$

$$\tag{129}$$

The decay rate is a result of the superposition of the free dipole radiation and the reflection from the nanofiber interface.

$$\Gamma \propto -\mathbf{d}\cdot\mathrm{Im}[\mathbf{G}(\mathbf{r}',\mathbf{r}')]\cdot\mathbf{d}^* \tag{130}$$

$$= \mathrm{tr}\left[(\mathbf{d}^*\mathbf{d})\cdot\mathrm{Im}[\mathbf{G}^*(\mathbf{r}',\mathbf{r}')]\right] \tag{131}$$

$$= \mathrm{tr}\left[\quad\cdot\mathrm{Im}[\mathbf{G}^*(\mathbf{r}',\mathbf{r}')]\right] \geq 0 \tag{132}$$

where $\quad = (\mathbf{d}^*\mathbf{d})$ is defined as the dipole orientation tensor which is merely a property of the atoms. The dyadic Green function part is only a property of the waveguide.

By mathematical definition, $\mathrm{Im}[\mathbf{G}^*(\mathbf{r}',\mathbf{r}')]$ is positive definite.

$$\mathrm{Im}[\mathbf{G}^*(\mathbf{r}',\mathbf{r}')] = \sum_{i=1,2,3} g_i\hat{\mathbf{v}}_i\hat{\mathbf{v}}_i, \text{ with } g_i > 0. \tag{133}$$

24

$\hat{\mathbf{v}}_i$ form the principal axes of the decay rate. The principal axes indicate the dipole orientations along which the interference between the free dipole radiation and the reflected field (equivalent to the radiation from the image dipole) is most constructive and destructive.

$$\Gamma = C(\omega) \sum_i g_i(\hat{\mathbf{v}}_i \cdot \quad \cdot \hat{\mathbf{v}}_i) = \sum_i (d_i')^2 g_i \tag{134}$$

$$= \Gamma_1 \cos^2 \phi \sin^2 \theta + \Gamma_2 \sin^2 \phi \sin^2 \theta + \Gamma_3 \cos^2 \theta, \tag{135}$$

where $d_i' = \sqrt{\hat{\mathbf{v}}_i \cdot \quad \cdot \hat{\mathbf{v}}_i}$ and $\mathbf{d}' = \sum_i d_i' \hat{\mathbf{v}}_i$ defines the equivalent dipole orientation of the atomic polarizability transition.

The range of decay rates:

$$\Gamma_1 = \Gamma_{max} \geq \Gamma(\theta, \phi) \geq \Gamma_{min} = \Gamma_3$$

Quantum transitions and dipole orientations correspondence:

$$\sigma_+ \leftrightarrow \mathbf{d}_+ \propto \frac{1}{\sqrt{2}} (i\mathbf{e}_{r_\perp} + \mathbf{e}_\phi) \tag{136}$$

$$\pi \leftrightarrow \mathbf{d}_0 \propto \mathbf{e}_z \tag{137}$$

$$\sigma_- \leftrightarrow \mathbf{d}_- \propto \frac{1}{\sqrt{2}} (-i\mathbf{e}_{r_\perp} + \mathbf{e}_\phi). \tag{138}$$
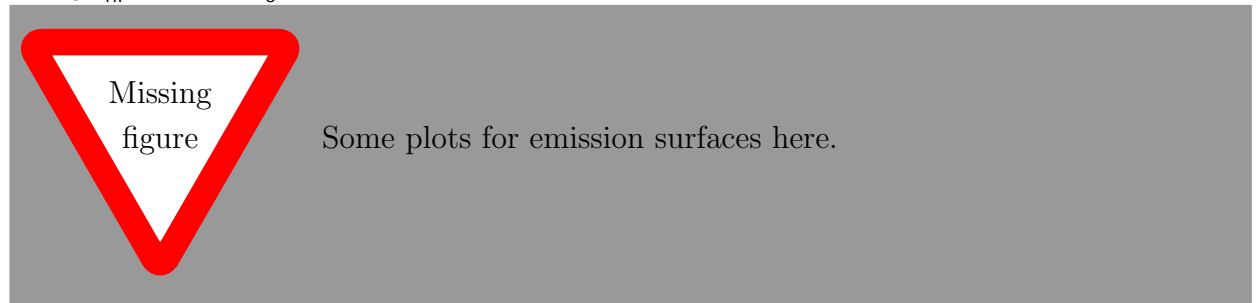
Example: completely mixed state decay rate calculation:

$$= \frac{1}{3} (\quad_+ + \quad_0 + \quad_-) = \frac{d_0^2}{3} \mathbf{I} \tag{139}$$

$$\Gamma = \frac{C(\omega)}{3} d_0^2 \mathrm{tr} \left[\mathrm{Im}[\mathbf{G}^*(\mathbf{r}', \mathbf{r}')] \right] = \frac{1}{3} (\Gamma_1 + \Gamma_2 + \Gamma_3). \tag{140}$$

This is equivalent to assume the dipole is uniformly pointing to any direction, and hence $\Gamma = \int \frac{}{4\pi} \Gamma(\theta, \phi) = \frac{1}{3}(\Gamma_1 + \Gamma_2 + \Gamma_3)$.

Missing figure

Some plots for emission surfaces here.

The phase shift is proportional to the time integral of the path on the emission rate surface. The range of the decay rates determines the achievable phase shift in a unit time.

However, the emission rate surface for the vacuum case is a uniform sphere and the corresponding phase shift in a given time is a constant independent from the orientation of the dipole with a scalar atomic polarizability. Therefore, it is possible to use the scalar atomic polarizability to realize a wide controllable phase shift range in the off-resonance regime that the vacuum configuration can hardly achieve.

C. Interference due to a one-sided or two-sided atom chain

Effect of an infinite long one-side chain... S matrix, reflectivity... Random filling effect...

To include many-atom interference effect, we can use the linear optical transformation matrix formalism. The transformation of modes should be the same for both Green function and Heisenberg picture approaches. Here, I am using the semiclassical Green function results first, and then the Heisenberg picture results.

From Equ. (21) and the results above, one can generalize the field transformation relationship due to the presence of an atom and an arbitrary incident mode $\mathbf{u}_{m'f'}(\mathbf{r})$ with mode amplitude $E_{m'f'}$ to give

$$\mathbf{E}^{out}(\mathbf{r}) = \sum_{mf} E_{mf}\mathbf{u}_{m'f'}(\mathbf{r}), \tag{141}$$

$$E_{mf} = \left[\delta_{mm'}\delta_{ff'} + C_{m'f'}^{mf}\right] E_{m'f'}, \tag{142}$$

with

$$C_{m'f'}^{mf} = i2\pi k_0 n_g \alpha \mathbf{u}^{mf*}(r'_\perp) \cdot \mathbf{u}_{m'f'}(r'_\perp) e^{i\beta_0(f'-f)z' + i(m'-m)\phi'}. \tag{143}$$

Therefore, one can define the scattering matrix $\mathbf{S} \equiv \left\{S_{m'f'}^{mf} | m, f, m', f' = \pm 1\right\}$ with elements $S_{m'f'}^{mf} = \delta_{mm'}\delta_{ff'} + C_{m'f'}^{mf}$.

Notice that, $\mathbf{r}' = (r'_\perp, \phi', z')$ indicates where the atom is sitting. If there are many atoms which are sitting at one transverse plane with the same z' position, one should sum over all those atom indexes to obtain the total scattering matrix at a z-slice. In our case, the atoms can sit at some random positions of either $\phi' = 0$ or $\phi' = \pi$ two sides of a periodic chain. For simplicity, we always use $z = z' = 0$ for the scattering matrix $\mathbf{S}(\phi')$ calculation on one z-slice. We define the free propagating transformation matrix, $\mathbf{P}(\Lambda) \equiv \left\{P_{m'f'}^{mf}(\Lambda) | m, f, m', f' = \pm 1\right\}$, by

$$P_{m'f'}^{mf}(\Lambda) = \delta_{mm'}\delta_{ff'}e^{if\beta_0} , \tag{144}$$

where Λ is the minimum distance or geometric period between atoms along the propagating direction of the guided light. The total field amplitude after the interaction with the last atom along the nanofiber due to the random occupied two-side chain of atoms can be given by

$$\left(E_{mf}^{out}\right) = [\eta_{N,+}\mathbf{S}(0) + \eta_{N,-}\mathbf{S}(\pi) + (1 - \eta_{N,+})(1 - \eta_{N,-})\mathbf{I}]\mathbf{P}(\Lambda)$$

$$[\eta_{N-1,+}\mathbf{S}(0) + \eta_{N-1,-}\mathbf{S}(\pi) + (1 - \eta_{N-1,+})(1 - \eta_{N-1,-})\mathbf{I}]\mathbf{P}(\Lambda)$$

$$\dots [\eta_{2,+}\mathbf{S}(0) + \eta_{2,-}\mathbf{S}(\pi) + (1 - \eta_{2,+})(1 - \eta_{2,-})\mathbf{I}]\mathbf{P}(\Lambda)$$

$$[\eta_{1,+}\mathbf{S}(0) + \eta_{1,-}\mathbf{S}(\pi) + (1 - \eta_{1,+})(1 - \eta_{1,-})\mathbf{I}]\left(E_{m'f'}^{in}\right) \tag{145}$$

$$= \left\{\prod_{i=N}^{2}[\eta_{i,+}\mathbf{S}(0) + \eta_{i,-}\mathbf{S}(\pi) + (1 - \eta_{i,+})(1 - \eta_{i,-})\mathbf{I}]\mathbf{P}(\Lambda)\right\}$$

$$[\eta_{1,+}\mathbf{S}(0) + \eta_{1,-}\mathbf{S}(\pi) + (1 - \eta_{1,+})(1 - \eta_{1,-})\mathbf{I}]\left(E_{m'f'}^{in}\right) \tag{146}$$

$$= \left\{\prod_{i=N}^{2}\mathbf{S}_i\mathbf{P}(\Lambda)\right\}\mathbf{S}_1\left(E_{m'f'}^{in}\right), \tag{147}$$

where $\mathbf{S}_i = \eta_{i,+}\mathbf{S}(0) + \eta_{i,-}\mathbf{S}(\pi) + (1 - \eta_{i,+})(1 - \eta_{i,-})\mathbf{I}$ denote the scattering matrix due to the randomly occupied atoms at the ith z-slice with random occupation variables $\eta_{i,\pm} = 0$ or 1 on both sides of the atom chain. The distribution of the random variables $\eta_{i,\pm}$ reflects how the atom chain is occupied.

For the case that both sides ($\phi' = 0$ and π) of the atom chain are fully occupied along the z-direction, the scattering matrix elements can be given by

$$S_{m'f'}^{mf} = 2\delta_{mm'}\delta_{ff'} + i2\pi k_0 n_g \alpha \mathbf{u}_{mf}^*(r_\perp') \cdot \mathbf{u}_{m'f'}(r_\perp')[1 + e^{i(m'-m)\pi}] \tag{148}$$

$$= 2\delta_{mm'}\delta_{ff'} + i2\pi k_0 n_g \alpha \left[|u_{r_\perp}(r_\perp')|^2 + mm'|u_\phi(r_\perp')|^2 + ff'|u_z(r_\perp')|^2\right][1 + e^{i(m'-m)\pi}] \tag{149}$$

$$= 2\delta_{mm'}\delta_{ff'} + i4\pi k_0 n_g \alpha \left[|u_{r_\perp}(r_\perp')|^2 + mm'|u_\phi(r_\perp')|^2 + ff'|u_z(r_\perp')|^2\right]. \tag{150}$$

We have treated the atomic polarizability as a scalar and used Born approximation here. Notice that, the polarization-dependent factor $[1 + e^{i(m'-m)\pi}]$ always yields 2 with $m, m' = \pm 1$ for the HE_{11} guided modes. If there are high-order guided modes, we expect to see destructive Birefringence effects for modes with odd modal index gaps.

This can also be understood by looking into the equations derived in the Heisenberg picture. The equivalent scattering matrix elements due to an atom positioned at $\mathbf{r}' =$

$(r'_\perp, \phi', z' = 0)$ can be obtained by making $t \to t_0$ from Equ. (62):

$$S^{mf}_{m'f'}(\phi') = \delta_{mm'}\delta_{ff'} - i\frac{2\pi g_\mu^*(\omega)g_{\mu'}(\omega)}{\Delta + i\Gamma/2} \tag{151}$$

$$= \delta_{mm'}\delta_{ff'} - i\frac{\frac{2\pi\omega}{v_g}\mathbf{u}^*_{mf}(\mathbf{r}'_\perp)\cdot\mathbf{d}_{ge}\mathbf{d}_{eg}\cdot\mathbf{u}_{m'f'}(\mathbf{r}'_\perp)e^{i(f'-f)\beta_0 z'}}{\Delta + i\Gamma/2} \tag{152}$$

$$= \delta_{mm'}\delta_{ff'} - i\frac{\frac{2\pi\omega}{v_g}\mathbf{u}^*_{mf}(r'_\perp)\cdot\mathbf{d}_{ge}\mathbf{d}_{eg}\cdot\mathbf{u}_{m'f'}(r'_\perp)e^{i(m'-m)\phi'}}{\Delta + i\Gamma/2}. \tag{153}$$

Therefore, the total scattering transformation matrix for the atom pair on both sides of the x-axis can be given by

$$S^{mf}_{m'f'}(\phi') = S^{mf}_{m'f'}(\phi' = 0) + S^{mf}_{m'f'}(\phi' = \pi) \tag{154}$$

$$= 2\delta_{mm'}\delta_{ff'} - i\frac{\frac{4\pi\omega}{v_g}\mathbf{u}^*_{mf}(r'_\perp)\cdot\mathbf{d}_{ge}\mathbf{d}_{eg}\cdot\mathbf{u}_{m'f'}(r'_\perp)}{\Delta + i\Gamma/2} \tag{155}$$

$$= 2\delta_{mm'}\delta_{ff'} - i4\pi k_0 n_g \mathbf{u}^*_{mf}(r'_\perp)\cdot \quad \cdot\mathbf{u}_{m'f'}(r'_\perp). \tag{156}$$

When $\beta_0 L$ is a multiple of π, the free propagation transformation matrix is proportional to a unitary matrix, and hence can be extracted out from the total transformation matrix formula (Equ. (147)). In that case, the total phase shift for a given input mode can be treated as the sum of the phase shift due to each individual atoms on both sides of the z-slices. Otherwise, there will be the asymmetric effect on the phase shifts of the forwarding and backwarding modes. Moreover, under the framework derived above, if we can ignore the backward propagating modes–which is approximately true if it is far from satisfying the geometric Bragg condition that $\beta_0\Lambda = n\pi$, the free propagating transformation matrix $\mathbf{P}(\Lambda)$ is also proportional to a unitary matrix, and hence the total phase shifts for individual forwarding modes can still be treated as a sum over all slices of atoms along the propagating direction. Physically, the asymmetric mixing of forward and backward propagating modes may be the major barrier to treat the total phase shift as the sum over all individual elements.

> Energy is not conserving under the Born approximation. How does the radiation power distribute after every event of scattering? A better model to explain what we should observe for the Birefringence effect.

IV. CONCLUSIONS

Appendix A: Radiation fields from an atom close to a nanofiber

As discussed in section II A, the 9 elements of a dyadic electric Green function is proportional to the local electric field components due to the radiation from an electric dipole orientated in some basis directions. The spontaneous radiation field components can be calculated through decomposing the field into reflected and transmitted field components and matching up the boundary conditions of the nanofiber which can be treated as an infinitely long cylindrical dielectric medium. The detailed calculations have been conducted by Nha, Klimov and others in their earlier publications [38, 39]. We summarize some of those results in this section.

One can separate the electric and magnetic fields into free-dipole radiation, reflected and transmitted parts. For example, the electric field can be written as

$$E(\mathbf{r}) = E^{(0)}(\mathbf{r}) + E^{(R)}(\mathbf{r}) + E^{(T)}(\mathbf{r}) \tag{A1}$$

$$= \begin{cases} E^{(0)}(\mathbf{r}) + E^{(R)}(\mathbf{r}), & r_\perp > a, \\ E^{(T)}(\mathbf{r}), & r_\perp \leq a. \end{cases} \tag{A2}$$

where the superscripts 0, R and T indicate the free-dipole radiation, reflection and transmission components of the field, and a is the radius of the nanofiber. For a translationally invariant waveguide, which means the index of refraction of the waveguide is independent of the propagating axis z, the electric and magnetic fields can be written as

$$E(\mathbf{r}) = E(\mathbf{r}_\perp)\exp(i\beta z), \qquad\qquad H(\mathbf{r}) = H(\mathbf{r}_\perp)\exp(i\beta z), \tag{A3}$$

where β is the propagation constant and $\mathbf{r}_\perp$ is the position vector in the transverse plane

29

perpendicular to the z-axis. We let the index of refraction of the nanofiber be

$$
n = n(r_\perp) = \begin{cases} n_2 = 1, & r_\perp > a, \\ \\ n_1, & r_\perp \le a. \end{cases} \tag{A4}
$$

To find the fields, we need to calculate the longitudinal components (the z-components) of the fields, and the transverse components can be obtained through z-components using the following relationships:

$$
\mathcal{E}_{r_\perp} = \frac{i}{\kappa_i^2} \left[\beta \frac{\partial \mathcal{E}_z}{\partial r_\perp} + \frac{k}{r_\perp} \frac{\partial \mathcal{H}_z}{\partial \phi} \right] = \frac{i\beta}{\kappa_i^2} \frac{\partial \mathcal{E}_z}{\partial r_\perp} - \frac{km}{r_\perp \kappa_i^2} \mathcal{H}_z, \tag{A5a}
$$

$$
\mathcal{E}_\phi = \frac{i}{\kappa_i^2} \left[\frac{\beta}{r_\perp} \frac{\partial \mathcal{E}_z}{\partial \phi} - k \frac{\partial \mathcal{H}_z}{\partial r_\perp} \right] = -\frac{\beta m}{r_\perp \kappa_i^2} \mathcal{E}_z - \frac{ik}{\kappa_i^2} \frac{\partial \mathcal{H}_z}{\partial r_\perp}, \tag{A5b}
$$

$$
\mathcal{H}_{r_\perp} = \frac{i}{\kappa_i^2} \left[\beta \frac{\partial \mathcal{H}_z}{\partial r_\perp} - \frac{kn^2}{r_\perp} \frac{\partial \mathcal{E}_z}{\partial \phi} \right] = \frac{i\beta}{\kappa_i^2} \frac{\partial \mathcal{H}_z}{\partial r_\perp} + \frac{kn^2 m}{r_\perp \kappa_i^2} \mathcal{E}_z, \tag{A5c}
$$

$$
\mathcal{H}_\phi = \frac{i}{\kappa_i^2} \left[\frac{\beta}{r_\perp} \frac{\partial \mathcal{H}_z}{\partial \phi} + kn^2 \frac{\partial \mathcal{E}_z}{\partial r_\perp} \right] = -\frac{\beta m}{r_\perp \kappa_i^2} \mathcal{H}_z + \frac{ikn^2}{\kappa_i^2} \frac{\partial \mathcal{E}_z}{\partial r_\perp} \tag{A5d}
$$

with $\kappa_i = \kappa_1$ or κ_2 and $n = n_1$ or n_2 for the corresponding space region. We use Gauss units in this paper, and assume the material of the nanofiber is non-magnetic, and hence $B = \mu_r H \approx H$ with the relative permeability $\mu_r \approx 1$. We have also defined the transverse propagation constant inside of the nanofiber, κ_1, by $\kappa_1^2 = n_1^2 k - \beta^2$. Similarly, one can define the transverse propagation constant outside of the nanofiber, κ_2, by $\kappa_2^2 = n_2^2 k - \beta^2 = k^2 - \beta^2$.

The longitudinal components of the electrical and magnetic fields can be expanded as Fourier transformations over the β space,

$$
\mathcal{E}_z^{(T)} = \sum_{m=-\infty}^{\infty} \int d\beta e^{im(\phi-\phi')+i\beta(z-z')} c_{m\beta} J_m(\kappa_1 r_\perp), \tag{A6a}
$$

$$
\mathcal{E}_z^{(0)} = \sum_{m=-\infty}^{\infty} \int d\beta e^{im(\phi-\phi')+i\beta(z-z')} \mathcal{E}_{z,m\beta}^{(0)}(r_\perp) \tag{A6b}
$$

$$
\mathcal{E}_z^{(R)} = \sum_{m=-\infty}^{\infty} \int d\beta e^{im(\phi-\phi')+i\beta(z-z')} a_{m\beta} H_m^{(1)}(\kappa_2 r_\perp), \tag{A6c}
$$

$$
\mathcal{B}_z^{(T)} = \sum_{m=-\infty}^{\infty} \int d\beta e^{im(\phi-\phi')+i\beta(z-z')} d_{m\beta} J_m(\kappa_1 r_\perp), \tag{A7a}
$$

$$
\mathcal{B}_z^{(0)} = \sum_{m=-\infty}^{\infty} \int d\beta e^{im(\phi-\phi')+i\beta(z-z')} \mathcal{B}_{z,m\beta}^{(0)}(r_\perp) \tag{A7b}
$$

30

$$\mathcal{B}_z^{(R)} = \sum_{m=-\infty}^{\infty} \int \mathrm{d}\beta e^{im(\phi-\phi')+i\beta(z-z')} b_{m\beta} H_m^{(1)}(\kappa_2 r_\perp), \tag{A7c}$$

in which J and H indicate the first kind of the Bessel function and the Hankel function as the cylindrical harmonics; the atom is positioned at $\mathbf{r}' = (r'_\perp, \phi', z')$ with an electric dipole moment $\mathbf{d}_0 = (d_{r_\perp}^0, d_\phi^0, d_z^0)$ in the atom's coordinate system. In the fiber's coordinate system, the dipole moment observed at an arbitrary position $\mathbf{r}$ is defined by the three components defined below:

$$d_{r_\perp} = \cos(\phi-\phi')d_{r_\perp}^0 + \sin(\phi-\phi')d_\phi^0 = \frac{1}{\sqrt{2}}\left(-e^{-i(\phi-\phi')}d_+ + e^{i(\phi-\phi')}d_-\right), \tag{A8}$$

$$d_\phi = \cos(\phi-\phi')d_\phi^0 - \sin(\phi-\phi')d_{r_\perp}^0 = \frac{i}{\sqrt{2}}\left(e^{-i(\phi-\phi')}d_+ + e^{i(\phi-\phi')}d_-\right), \tag{A9}$$

$$d_z = d_z^0, \tag{A10}$$

where we have defined the position-independent reduced dipole components

$$d_\pm \equiv \mp\frac{1}{\sqrt{2}}(d_{r_\perp}^0 \pm id_\phi^0). \tag{A11}$$

The terms associated with $d_\pm$ in the dipole moment formula lower or raise the mode index or the angular momentum quantum number, m, of the interacting fiber modes by 1. Notice that we have used $\phi-\phi'$ as the projected angle between $\mathbf{r}$ and $\mathbf{r}'$ on the transverse plane to make the relationship valid in general. In most of our calculations, we usually position the atom on the x-axis of the fiber coordinate and set $z' = 0$.

The free radiation field components associated with the $e^{im(\phi-\phi')+i\beta(z-z')}$ term (the m-th mode components) for the $r_\perp < r'_\perp$ region can be given by

$$\mathcal{B}_{z,m\beta}^{(0)} = \frac{ik\kappa_2}{2\sqrt{2}}J_m(pr_\perp)\left[d_+H_{m+1}^{(1)}(\kappa_2 r'_\perp) - d_-H_{m-1}^{(1)}(\kappa_2 r'_\perp)\right], \tag{A12}$$

$$\mathcal{B}_{\phi,m\beta}^{(0)} = \frac{ik}{2}\left[\frac{\beta d_-}{\sqrt{2}}J_{m-1}(\kappa_2 r_\perp)H_{m-1}^{(1)}(\kappa_2 r'_\perp) - \frac{\beta d_+}{\sqrt{2}}J_{m+1}(\kappa_2 r_\perp)H_{m+1}^{(1)}(\kappa_2 r'_\perp)\right.$$
$$\left.+\frac{i\kappa_2 d_z^0}{2}(J_{m-1}(\kappa_2 r_\perp) - J_{m+1}(\kappa_2 r_\perp))H_m^{(1)}(\kappa_2 r'_\perp)\right], \tag{A13}$$

$$\mathcal{B}_{r_\perp,m\beta}^{(0)} = \frac{k}{2}\left[\frac{imd_z^0}{r_\perp}J_m(\kappa_2 r_\perp)H_m^{(1)}(\kappa_2 r'_\perp)\right.$$
$$\left.+\frac{\beta d_+}{\sqrt{2}}J_{m+1}(\kappa_2 r_\perp)H_{m+1}^{(1)}(\kappa_2 r'_\perp) + \frac{\beta d_-}{\sqrt{2}}J_{m-1}(\kappa_2 r_\perp)H_{m-1}^{(1)}(\kappa_2 r'_\perp)\right], \tag{A14}$$

$$\mathcal{E}_{z,m\beta}^{(0)} = \frac{\kappa_2}{2}J_m(\kappa_2 r_\perp)\left[id_z^0\kappa_2 H_m^{(1)}(\kappa_2 r'_\perp)\right.$$

$$+\frac{\beta d_+}{\sqrt{2}}H_{m+1}^{(1)}\left(\kappa_2 r'_\perp\right)+\frac{\beta d_-}{\sqrt{2}}H_{m-1}^{(1)}\left(\kappa_2 r'_\perp\right)\bigg], \tag{A15}$$

$$\mathcal{E}_{\phi,m\beta}^{(0)}=-\frac{im\beta d_z^0}{2r_\perp}J_m\left(\kappa_2 r_\perp\right)H_m^{(1)}\left(\kappa_2 r'_\perp\right)$$
$$+\frac{d_+}{2\sqrt{2}}\left[\frac{m\kappa_2}{r_\perp}J_m\left(\kappa_2 r_\perp\right)-k^2 J_{m+1}\left(\kappa_2 r_\perp\right)\right]H_{m+1}^{(1)}\left(\kappa_2 r'_\perp\right)$$
$$+\frac{d_-}{2\sqrt{2}}\left[\frac{m\kappa_2}{r_\perp}J_m(\kappa_2 r_\perp)-k^2 J_{m-1}(\kappa_2 r_\perp)\right]H_{m-1}^{(1)}(\kappa_2 r'_\perp), \tag{A16}$$

$$\mathcal{E}_{r_\perp,m\beta}^{(0)}=\frac{\beta\kappa_2 d_z^0}{4}\left[J_{m+1}(\kappa_2 r_\perp)-J_{m-1}(\kappa_2 r_\perp)\right]H_m^{(1)}\left(\kappa_2 r'_\perp\right)$$
$$-\frac{d_+}{2\sqrt{2}}\left[i\beta^2 J_{m+1}(\kappa_2 r_\perp)+\frac{im\kappa_2}{r_\perp}J_m(\kappa_2 r_\perp)\right]H_{m+1}^{(1)}(\kappa_2 r'_\perp)$$
$$+\frac{d_-}{2\sqrt{2}}\left[i\beta^2 J_{m-1}(\kappa_2 r_\perp)+\frac{im\kappa_2}{r_\perp}J_m(\kappa_2 r_\perp)\right]H_{m-1}^{(1)}(\kappa_2 r'_\perp). \tag{A17}$$

The magnetic and electrical fields components for $r_\perp > r'_\perp$ are

$$\mathcal{B}_{z,m\beta}^{(0)}=\frac{ik\kappa_2}{2\sqrt{2}}H_m^{(1)}(\kappa_2 r_\perp)\left[d_+ J_{m+1}(\kappa_2 r'_\perp)-d_- J_{m-1}(\kappa_2 r'_\perp)\right], \tag{A18}$$

$$\mathcal{B}_{\phi,m\beta}^{(0)}=\frac{ik}{2}\left[\frac{\beta d_-}{\sqrt{2}}H_{m-1}^{(1)}\left(\kappa_2 r_\perp\right)J_{m-1}\left(\kappa_2 r'_\perp\right)-\frac{\beta d_+}{\sqrt{2}}H_{m+1}^{(1)}\left(\kappa_2 r_\perp\right)J_{m+1}\left(\kappa_2 r'_\perp\right)\right.$$
$$\left.+\frac{i\kappa_2 d_z^0}{2}\left(H_{m-1}^{(1)}(\kappa_2 r_\perp)-H_{m+1}^{(1)}(\kappa_2 r_\perp)\right)J_m(\kappa_2 r'_\perp)\right], \tag{A19}$$

$$\mathcal{B}_{r_\perp,m\beta}^{(0)}=\frac{k}{2}\left[\frac{imd_z^0}{r_\perp}H_m^{(1)}\left(\kappa_2 r_\perp\right)J_m\left(\kappa_2 r'_\perp\right)\right.$$
$$\left.+\frac{\beta d_+}{\sqrt{2}}H_{m+1}^{(1)}(\kappa_2 r_\perp)J_{m+1}(\kappa_2 r'_\perp)+\frac{\beta d_-}{\sqrt{2}}H_{m-1}^{(1)}(\kappa_2 r_\perp)J_{m-1}(\kappa_2 r'_\perp)\right], \tag{A20}$$

$$\mathcal{E}_{z,m\beta}^{(0)}=\frac{\kappa_2}{2}H_m^{(1)}\left(\kappa_2 r_\perp\right)\left[id_z^0\kappa_2 J_m\left(\kappa_2 r'_\perp\right)\right.$$
$$\left.+\frac{\beta d_+}{\sqrt{2}}J_{m+1}\left(\kappa_2 r'_\perp\right)+\frac{\beta d_-}{\sqrt{2}}J_{m-1}\left(\kappa_2 r'_\perp\right)\right], \tag{A21}$$

$$\mathcal{E}_{\phi,m\beta}^{(0)}=-\frac{im\beta d_z^0}{2r_\perp}H_m^{(1)}\left(\kappa_2 r_\perp\right)J_m\left(\kappa_2 r'_\perp\right)$$
$$+\frac{d_+}{2\sqrt{2}}\left[\frac{m\kappa_2}{r_\perp}H_m^{(1)}\left(\kappa_2 r_\perp\right)-k^2 H_{m+1}^{(1)}\left(\kappa_2 r_\perp\right)\right]J_{m+1}\left(\kappa_2 r'_\perp\right)$$
$$+\frac{d_-}{2\sqrt{2}}\left[\frac{m\kappa_2}{r_\perp}H_m^{(1)}(\kappa_2 r_\perp)-k^2 H_{m-1}^{(1)}(\kappa_2 r_\perp)\right]J_{m-1}(\kappa_2 r'_\perp), \tag{A22}$$

$$\mathcal{E}_{r_\perp,m\beta}^{(0)}=\frac{\beta\kappa_2 d_z^0}{4}\left[H_{m+1}^{(1)}(\kappa_2 r_\perp)-H_{m-1}^{(1)}(\kappa_2 r_\perp)\right]J_m\left(\kappa_2 r'_\perp\right)$$
$$-\frac{d_+}{2\sqrt{2}}\left[i\beta^2 H_{m+1}^{(1)}(\kappa_2 r_\perp)+\frac{im\kappa_2}{r_\perp}H_m^{(1)}(\kappa_2 r_\perp)\right]J_{m+1}(\kappa_2 r'_\perp)$$
$$+\frac{d_-}{2\sqrt{2}}\left[i\beta^2 H_{m-1}^{(1)}(\kappa_2 r_\perp)+\frac{im\kappa_2}{r_\perp}H_m^{(1)}(\kappa_2 r_\perp)\right]J_{m-1}(\kappa_2 r'_\perp). \tag{A23}$$

By using the boundary conditions at $r_\perp = a$ and Equ. (A2) that

$$\mathcal{E}_z(r_\perp = a^>) = \mathcal{E}_z(r_\perp = a^<), \tag{A24}$$

$$\mathcal{B}_z(r_\perp = a^>) = \mathcal{B}_z(r_\perp = a^<), \tag{A25}$$

$$\mathcal{E}_\phi(r_\perp = a^>) = \mathcal{E}_\phi(r_\perp = a^<), \tag{A26}$$

$$\mathcal{B}_\phi(r_\perp = a^>) = \mathcal{B}_\phi(r_\perp = a^<), \tag{A27}$$

where $a^<$ and $a^>$ denote the boundaries at the sides less and larger than a, and the connections between field components (Equ. (A5)), we can obtain all unknown coefficients. To summarize, we have [38]

$$a_{m\beta} = \frac{na}{P^2 + QR}, \tag{A28}$$

$$b_{m\beta} = \frac{nb}{P^2 + QR}, \tag{A29}$$

$$c_{m\beta} = \frac{\mathcal{E}_{z,m\beta}^{(0)}(r_\perp = a) + H_m^{(1)}(\kappa_2 a) a_{m\beta}}{J_m(\kappa_1 a)}, \tag{A30}$$

$$d_{m\beta} = \frac{\mathcal{H}_{z,m\beta}^{(0)}(r_\perp = a) + H_m^{(1)}(\kappa_2 a) b_{m\beta}}{J_m(\kappa_1 a)}, \tag{A31}$$

where

$$\begin{aligned}
na &= \kappa_1^2 \kappa_2^2 a J_m(\kappa_1 a) P E_{\phi,m\beta}^{(0)}(r_\perp = a) \\
&\quad + \kappa_2^2 \left[J_m(\kappa_1 a) \beta m P + k a n_1^2 \kappa_1 \frac{\mathrm{d}}{\mathrm{d}(\kappa_1 a)} J_m(\kappa_1 a) Q \right] E_{z,m\beta}^{(0)} \\
&\quad + i \kappa_1^2 \kappa_2^2 a J_m(\kappa_1 a) Q B_{\phi,m\beta}^{(0)}(r_\perp = a) - i m \beta \kappa_1 \kappa_2 J_m(\kappa_1 a) S B_{z,m\beta}^{(0)}(r_\perp = a), \tag{A32}
\end{aligned}$$

$$\begin{aligned}
nb &= \kappa_1^2 \kappa_2^2 a J_m(\kappa_1 a) P B_{\phi,m\beta}^{(0)}(r_\perp = a) \\
&\quad + \kappa_2^2 \left[J_m(\kappa_1 a) \beta m P - k a \kappa_1 \frac{\mathrm{d}}{\mathrm{d}(\kappa_1 a)} J_m(\kappa_1 a) R \right] B_{z,m\beta}^{(0)} \\
&\quad + i \kappa_1^2 \kappa_2^2 a J_m(\kappa_1 a) R E_{\phi,m\beta}^{(0)}(r_\perp = a) + i m \beta \kappa_1 \kappa_2 J_m(\kappa_1 a) T E_{z,m\beta}^{(0)}(r_\perp = a), \tag{A33}
\end{aligned}$$

and

$$P = m \beta k^2 J_m(\kappa_1 a) H_m^{(1)}(\kappa_2 a)(n_1^2 - 1), \tag{A34}$$

$$Q = -\kappa_1 \kappa_2 a k \left[\kappa_1 J_m(\kappa_1 a) \frac{\mathrm{d}}{\mathrm{d}(\kappa_2 a)} H_m^{(1)}(\kappa_2 a) - \kappa_2 H_m^{(1)}(\kappa_2 a) \frac{\mathrm{d}}{\mathrm{d}(\kappa_1 a)} J_m(\kappa_1 a) \right], \tag{A35}$$

$$R = \kappa_1 \kappa_2 a k \left[\kappa_1 J_m(\kappa_1 a) \frac{\mathrm{d}}{\mathrm{d}(\kappa_2 a)} H_m^{(1)}(\kappa_2 a) - \kappa_2 n_1^2 H_m^{(1)}(\kappa_2 a) \frac{\mathrm{d}}{\mathrm{d}(\kappa_1 a)} J_m(\kappa_1 a) \right], \tag{A36}$$

$$S = \kappa_1 \kappa_2 a k \left[\kappa_2 J_m(\kappa_1 a) \frac{\mathrm{d}}{\mathrm{d}(\kappa_2 a)} H_m^{(1)}(\kappa_2 a) - \kappa_1 H_m^{(1)}(\kappa_2 a) \frac{\mathrm{d}}{\mathrm{d}(\kappa_1 a)} J_m(\kappa_1 a) \right], \qquad (A37)$$

$$T = \kappa_1 \kappa_2 a k \left[\kappa_2 J_m(\kappa_1 a) \frac{\mathrm{d}}{\mathrm{d}(\kappa_2 a)} H_m^{(1)}(\kappa_2 a) - \kappa_1 n_1^2 H_m^{(1)}(\kappa_2 a) \frac{\mathrm{d}}{\mathrm{d}(\kappa_1 a)} J_m(\kappa_1 a) \right]. \qquad (A38)$$

The integral in Equs. (A5) should be chosen along path C_1 as shown in Fig. 3 to detour the branch cuts and singularities of integrands. The branch cuts are determined by $\mathrm{Im}[\kappa_2], \mathrm{Im}[\kappa_1] > 0$ to ensure the integrands single-valued and remain on the Riemann sheet where the radiation fields decrease at the infinities. Note that there are only two branch cuts along the y-axis and within $[-n_2 k, n_2 k]$ on the x-axis originated from $\mathrm{Im}[\kappa_2] = 0$. The $\mathrm{Im}[\kappa_1] = 0$ condition does not yield any other new branch cuts where the integrands discontinue. Approximately, we use dashed lines to indicate the branch cuts on the left subplots in Fig. 3. There are also poles on the complex plane of β, and are located at $\pm \beta_0$ characterizing the guided modes (HE_{11} modes for the single-mode nanofiber). We exclude the singularities by closing the integration contours on the upper-half complex plane of β when $z > 0$ and the lower-half plane when $z < 0$ to ensure the Fourier transform convergent at infinities. Since the closed contour integrals vanish, the integrals along C_1 can be transformed to the contour integrals detouring the branch cuts and around the poles which correspond to the radiation mode and the guided mode components, respectively. We have used the fact that the integrands vanish at infinities (red solid contour paths). Along the contour paths, we choose κ_1 always positive real while κ_2 being negative real in the first and third quadrants and being positive real in the second and forth quadrants.

More information: Physics meaning of the sections detouring the branch cuts and poles... The integrals along the vertical sections of the contour paths, a and d, cancel. The integrals along the horizontal sections, b and c, double one the other. In the end, the contour integral detouring the branch cuts yields $2 \int_0^k \mathrm{d}\beta$ for $z > 0$ or $2 \int_{-k}^0 \mathrm{d}\beta$ for $z < 0$ with $n_2 = 1$. Similarly, one can show that the contour integrals around the poles with separated segments of positive and negative real κ_2's are equivalent to $\pm 2 \oint_{\pm \beta_0} \mathrm{d}\beta$ with positive real κ_2. When $z = 0$, the full integral along path C_1 can be rewritten as the average value of the $z > 0$ and $z < 0$ limits. Therefore, we have

$$\int_{C_1} \mathrm{d}\beta = \int_{-k}^k \mathrm{d}\beta + \oint_{\beta_0} \mathrm{d}\beta - \oint_{-\beta_0} \mathrm{d}\beta, \qquad (A39)$$

where the first integral yield the radiation mode contribution and the last two terms yield the guided mode contribution in two respective propagation directions. When we calculate
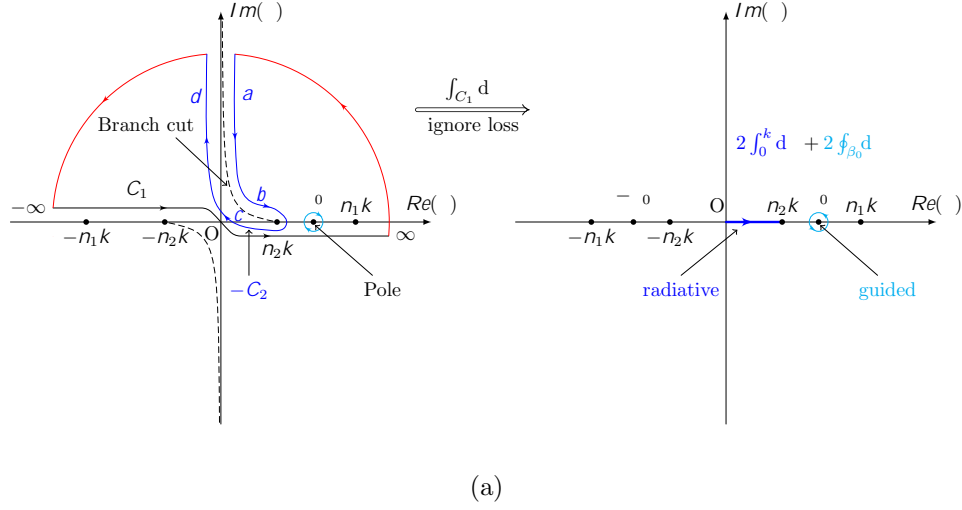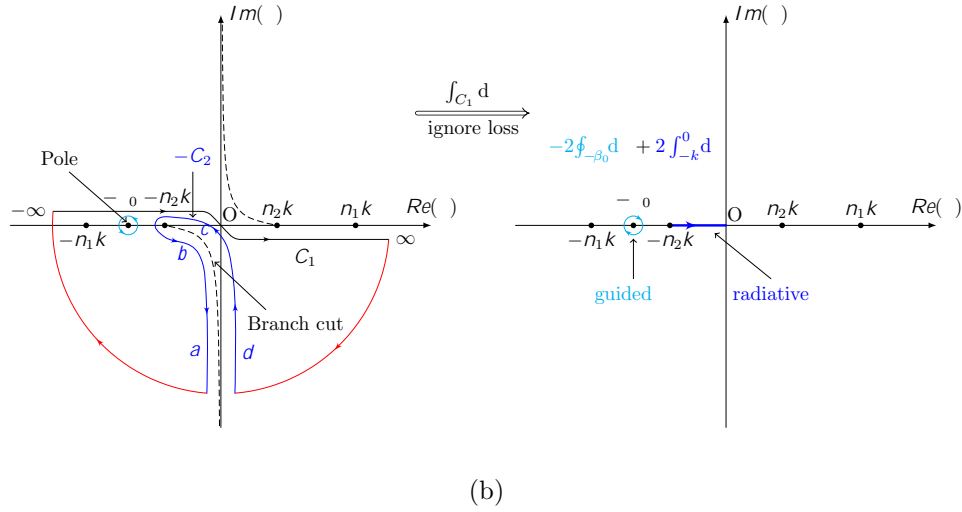
FIG. 3: Equivalent integration paths to calculate the radiation and guided fields. For $z > 0$, we can use the zero-valued contour integral path drawn in subfig. 3a to calculate the integration along path C_1. The simplified integration path by ignoring waveguide losses is given in the top-right plot. It only contains the forward propagating mode contributions with radiation and guided mode components as divided through the real-axis integral and the residual of the pole. For the $z < 0$ case, the contour integral analysis is given in subfig. 3b, which only includes the backward propagating mode contributions.

the decay rates or phase shift due to the presence of atoms along a nanofiber, we can use this decomposition relationship of integrals. Notice that, the guided mode contribution part should only include the $m = \pm 1$ HE_{11} modes when summing over mode index m for a single-mode nanofiber.

Appendix B: Group index of refraction and mode functions of the fundamental guided modes

The longitudinal propagation constant β_0 of the fundamental HE_{11} guided mode is the solution of β determined by the fiber eigenvalue equation [18]

$$f(\kappa_1, q, k, \beta) = 0, \tag{B1}$$

where

$$f(\kappa_1, q, k, \beta) = \frac{J_0(\kappa_1 a)}{\kappa_1 a J_1(\kappa_1 a)} + \frac{n_1^2 + n_2^2}{2n_1^2} \frac{K_1'(qa)}{qa K_1(qa)} - \frac{1}{\kappa_1^2 a^2} \tag{B2}$$

$$+ \left\{ \left[\frac{n_1^2 - n_2^2}{2n_1^2} \frac{K_1'(qa)}{qa K_1(qa)} \right]^2 + \frac{\beta^2}{n_1^2 k^2} \left(\frac{1}{q^2 a^2} + \frac{1}{\kappa_1^2 a^2} \right)^2 \right\}^{1/2} \tag{B3}$$

and the transverse propagation constants $\kappa_1 = \sqrt{n_1^2 k^2 - \beta^2}$ and $q = \sqrt{\beta^2 - n_2^2 k^2} = \sqrt{\beta^2 - k^2}$. J_n and K_n stand for the Bessel functions of the first kind and the modified Bessel functions of the second kind, respectively.

We differentiate the fiber eigenvalue equation above with respect to β on both sides, and obtain

$$\frac{\mathrm{d}f}{\mathrm{d}\beta} = \frac{\partial f}{\partial \kappa_1} \left(\frac{\partial \kappa_1}{\partial k} \frac{\mathrm{d}k}{\mathrm{d}\beta} + \frac{\partial \kappa_1}{\partial \beta} \right) + \frac{\partial f}{\partial q} \left(\frac{\partial q}{\partial k} \frac{\mathrm{d}k}{\mathrm{d}\beta} + \frac{\partial q}{\partial \beta} \right) + \frac{\partial f}{\partial k} \frac{\mathrm{d}k}{\mathrm{d}\beta} + \frac{\partial f}{\partial \beta} = 0 \tag{B4}$$

Therefore, the group index of refraction of the fundamental modes of the nanofiber can be given by

$$n_g = \frac{\mathrm{d}\beta}{\mathrm{d}k} = -\frac{\frac{\partial f}{\partial \kappa_1} \frac{\partial \kappa_1}{\partial k} + \frac{\partial f}{\partial q} \frac{\partial q}{\partial k} + \frac{\partial f}{\partial k}}{\frac{\partial f}{\partial \kappa_1} \frac{\partial \kappa_1}{\partial \beta} + \frac{\partial f}{\partial q} \frac{\partial q}{\partial \beta} + \frac{\partial f}{\partial \beta}}. \tag{B5}$$

Missing figure

Frequency stability, linearity and maybe other aspects of the group index of refraction.

The fundamental mode functions, $\mathbf{u}^{(\mu)}(r_\perp, \phi, z)$, of the electric components of the fiber [18, 44] can be separated into $r_\perp-$, $\phi-$ and $z-$dependent parts, and are characterized by the

36

mode index $\mu = (\beta_0, f, \xi)$, where $f = \pm 1$ indicates forward and backward propagating directions and ξ indicates the polarization state of the mode. For a quasicircularly polarized fundamental mode, we use $\xi = m = \pm$ to indicate the counterclockwise and clockwise rotations, respectively; for a quasilinearly polarized fundamental mode, we usually use $\xi = \phi_0$ to indicate the rotation angle, ϕ_0, of the polarization axis from the x-axis; specially, we use $\xi = H$ or V when the quasilinear polarization axis is along the x-axis or y-axis, respectively. For the circularly polarized case, the fundamental mode can be written as

$$\mathbf{u}^{(\mu)}(r_\perp, \phi, z) = u_{r_\perp}^{(\mu)}(r_\perp)e^{if\beta_0 z + im\phi}\hat{r}_\perp + u_\phi^{(\mu)}(r_\perp)e^{if\beta_0 z + im\phi}\hat{\phi} + u_z^{(\mu)}(r_\perp)e^{if\beta_0 z + im\phi}\hat{z} \quad \text{(B6)}$$

$$= u_{r_\perp}(r_\perp)e^{if\beta_0 z + im\phi}\hat{r}_\perp + mu_\phi(r_\perp)e^{if\beta_0 z + im\phi}\hat{\phi} + fu_z(r_\perp)e^{if\beta_0 z + im\phi}\hat{z}, \quad \text{(B7)}$$

where the forwarding, counterclockwise rotating guided mode components, $\mathbf{u}(r_\perp)$, are determined, for $r_\perp < a$, by

$$u_{r_\perp}(r_\perp) = -A\frac{\beta_0}{2\kappa_1}\left[(1-s)J_0(\kappa_1 r_\perp) - (1+s)J_2(\kappa_1 r_\perp)\right] \quad \text{(B8a)}$$

$$u_\phi(r_\perp) = -imA\frac{\beta_0}{2\kappa_1}\left[(1-s)J_0(\kappa_1 r_\perp) + (1+s)J_2(\kappa_1 r_\perp)\right] \quad \text{(B8b)}$$

$$u_z(r_\perp) = ifAJ_1(\kappa_1 r_\perp), \quad \text{(B8c)}$$

and, for $r_\perp > a$, by

$$u_{r_\perp}(r_\perp) = -A\frac{\beta_0}{2\kappa_1}\frac{J_1(\kappa_1 a)}{K_1(qa)}\left[(1-s)K_0(qr_\perp) + (1+s)K_2(qr_\perp)\right] \quad \text{(B9a)}$$

$$u_\phi(r_\perp) = -imA\frac{\beta_0}{2\kappa_1}\frac{J_1(\kappa_1 a)}{K_1(qa)}\left[(1-s)K_0(qr_\perp) - (1+s)K_2(qr_\perp)\right] \quad \text{(B9b)}$$

$$u_z(r_\perp) = ifA\frac{J_1(\kappa_1 a)}{K_1(qa)}K_1(qr_\perp), \quad \text{(B9c)}$$

with

$$s = \left[\frac{1}{(\kappa_1 a)^2} + \frac{1}{(qa)^2}\right]\left[\frac{J_1'(\kappa_1 a)}{\kappa_1 aJ_1(\kappa_1 a)} + \frac{K_1'(qa)}{qaK_1(qa)}\right], \quad \text{(B10)}$$

$$\kappa_1 = \sqrt{k^2 n_1^2 - \beta_0^2}. \quad \text{(B11)}$$

The normalization factor, A, is determined by the normalized energy that

$$1 = \int_0^{2\pi} d\phi \int_0^\infty dr_\perp r_\perp\, n^2(\mathbf{r}_\perp)|E^g(\mathbf{r}_\perp)|^2 = 2\pi A^2 a^2(n_1^2 P_1 + n_2^2 P_2), \quad \text{(B12)}$$

where the stored energy distribution factors are

$$P_1 = \frac{\beta_0^2}{4\kappa_1^2}\left\{(1-s)^2\left[J_0^2(\kappa_1 a) + J_1^2(\kappa_1 a)\right] + (1+s)^2\left[J_2^2(\kappa_1 a) - J_1(\kappa_1 a)J_3(\kappa_1 a)\right]\right\}$$

37

$$+ \frac{1}{2}\left[J_1^2(\kappa_1 a) - J_0(\kappa_1 a)J_2(\kappa_1 a)\right] \tag{B13}$$

$$P_2 = \frac{\beta_0^2 J_1^2(\kappa_1 a)}{4q^2 K_1^2(qa)}\left\{(1-s)^2\left[K_1^2(qa) - K_0^2(qa)\right]\right.$$

$$\left. +(1+s)^2\left[K_1(qa)K_3(qa) - K_2^2(qa)\right] + \frac{2q^2}{\beta^2}\left[K_0(qa)K_2(qa) - K_1^2(qa)\right]\right\}. \tag{B14}$$

Using this basis, the electric part of a guided field with quasicircularly propagating mode index $\mu = (\beta_0, f, m)$ can be written as

$$E^{(\mu)}(r_\perp, \phi, z, t) = E_0\left[u_{r_\perp}(r_\perp)\hat{r}_\perp + mu_\phi(r_\perp)\hat{\phi} + fu_z(r_\perp)\hat{z}\right]e^{if\beta_0 z + im\phi - i\omega t}. \tag{B15}$$

The power propagating inside and outside the fiber can be given in terms of the time averaged Poynting vector along the propagation direction, $\langle S_z \rangle$, by

$$P_{in} = \int_0^{2\pi} \mathrm{d}\phi \int_0^a \langle S_z \rangle\, r_\perp \mathrm{d}r_\perp \tag{B16}$$

$$P_{out} = \int_0^{2\pi} \mathrm{d}\phi \int_a^\infty \langle S_z \rangle\, r_\perp \mathrm{d}r_\perp. \tag{B17}$$

The total power $P = P_{in} + P_{out}$. One can show that the normalization constant $E_0 A$ reads

$$E_0 A = \sqrt{\frac{4\mu_0 \omega P}{\pi a^2 \beta_0}}\,(D_{in} + D_{out})^{-1/2}, \tag{B18}$$

where

$$D_{in} = (1-s)\left[1 + (1-s)\frac{\beta_0^2}{\kappa_1^2}\right]\left(J_0^2(\kappa_1 a) + J_1^2(\kappa_1 a)\right)$$

$$+ (1+s)\left[1 + (1+s)\frac{\beta_0^2}{\kappa_1^2}\right]\left(J_2^2(\kappa_1 a) - J_1(\kappa_1 a)J_3(\kappa_1 a)\right) \tag{B19}$$

$$D_{out} = \frac{J_1^2(\kappa_1 a)}{K_1^2(qa)}\left\{(1-s)\left[1 - (1-s)\frac{\beta_0^2}{q^2}\right]\left(K_0^2(qa) - K_1^2(qa)\right)\right.$$

$$\left. +(1+s)\left[1 - (1+s)\frac{\beta_0^2}{q^2}\right]\left(K_2^2(qa) - K_1(qa)K_3(qa)\right)\right\}. \tag{B20}$$

For a quasilinearly polarized fundamental guided mode, the electric part of the mode can be written as

$$\mathbf{u}^{(\beta_0, f, \phi_0)}(r_\perp, \phi, z) = \frac{1}{\sqrt{2}}\left(\mathbf{u}^{(\beta_0, f, +)}(r_\perp, \phi, z)e^{-i\phi_0} + \mathbf{u}^{(\beta_0, f, -)}(r_\perp, \phi, z)e^{i\phi_0}\right) \tag{B21}$$

$$= \sqrt{2}\left[u_{r_\perp}(r_\perp)\cos(\phi - \phi_0)\hat{\mathbf{r}}_\perp + iu_\phi(r_\perp)\sin(\phi - \phi_0)\hat{}\right.$$

$$\left. +fu_z(r_\perp)\cos(\phi - \phi_0)\hat{\mathbf{z}}\right]e^{if\beta_0 z}. \tag{B22}$$

One can write down an arbitrary quasilinearly polarized electric field in the form similar to the quasicircularly polarized case with $E_0 A$ satisfying the same relationship defined in Equ. (B18).

Particularly, when $\phi_0 = 0$ and $\pi/2$, we obtain the H and V fundamental modes as

$$\mathbf{u}^{(\beta_0, f, H)}(r_\perp, \phi, z) = \sqrt{2}\left[u_{r_\perp}(r_\perp)\cos(\phi)\hat{\mathbf{r}}_\perp + iu_\phi(r_\perp)\sin(\phi)\,\hat{}\; + fu_z(r_\perp)\cos(\phi)\hat{\mathbf{z}}\right]e^{if\beta_0 z} \quad \text{(B23)}$$

$$\mathbf{u}^{(\beta_0, f, V)}(r_\perp, \phi, z) = \sqrt{2}\left[u_{r_\perp}(r_\perp)\sin(\phi)\hat{\mathbf{r}}_\perp - iu_\phi(r_\perp)\cos(\phi)\,\hat{}\; + fu_z(r_\perp)\sin(\phi)\hat{\mathbf{z}}\right]e^{if\beta_0 z}. \quad \text{(B24)}$$

To show $v_g = \frac{P}{W}$ using the formulas above?

Appendix C: Light-atom interaction in the dispersive regime

Detailed derivation can be found in Qi's hand-written notes on *Dispersive eld-atom interaction Hamiltonian*. The special case of a single mode propagating in a homogeneous medium can be found in Ben's dissertation (chapter 4).

The dispersive light shift interaction describes an atom's effective response to an electric field when the excited states can be adiabatically eliminated from the quantum dynamics. This reduced description applies when the saturation parameter of atoms is much smaller than 1:

$$s = \frac{\Omega^2/4}{\Delta^2 + \Gamma^2/4} \ll 1, \quad \text{(C1)}$$

where Ω is the Rabi frequency, Γ is the total spontaneous emission rate of the atoms, and $\Delta = \omega_0 - \omega_{eg}$ is the probe detuning from the atomic resonance frequency ω_{eg} of the given excited and ground states. As the saturation parameter is proportional to the ratio of the Rabi frequency to the detuning, Ω/Δ, physically this allows condition Eq. (C1) to be satisfied even for large driving power (Rabi frequency) as long as the probe laser is far enough detuned. In this limit, the atom-light coupling can be described by the dispersive light-shift interaction,

$$
\begin{aligned}
\hat{H}_{\mathrm{e}} &= \sum_{f,f'=\pm 1}\hat{H}_{\mathrm{e}}^{ff'} = -\sum_{f,f'=\pm 1}\hat{\mathbf{E}}_f^{(-)}(\mathbf{r}') \cdot \quad \cdot \hat{\mathbf{E}}_{f'}^{(+)}(\mathbf{r}') &\text{(C2)}\\
&= -\hat{\mathbf{E}}_+^{(-)}(\mathbf{r}') \cdot \quad \cdot \hat{\mathbf{E}}_+^{(+)}(\mathbf{r}') - \hat{\mathbf{E}}_+^{(-)}(\mathbf{r}') \cdot \quad \cdot \hat{\mathbf{E}}_-^{(+)}(\mathbf{r}')\\
&\quad - \hat{\mathbf{E}}_-^{(-)}(\mathbf{r}') \cdot \quad \cdot \hat{\mathbf{E}}_+^{(+)}(\mathbf{r}') - \hat{\mathbf{E}}_-^{(-)}(\mathbf{r}') \cdot \quad \cdot \hat{\mathbf{E}}_-^{(+)}(\mathbf{r}'), &\text{(C3)}
\end{aligned}
$$

where the electric field operator is evaluated at the atomic position $\mathbf{r}'$, and the electric component of the guided field can be given by

$$\hat{\mathbf{E}} = (\hat{\mathbf{E}}^{(+)}e^{-i\omega_0 t} + c.c.)/2 \tag{C4}$$

with

$$\hat{\mathbf{E}}^{(+)}(\mathbf{r}) = \sum_{f=\pm 1} \hat{\mathbf{E}}_f^{(+)}(\mathbf{r}) = \sqrt{\frac{2\pi\hbar\omega_0}{v_g\tau}} \sum_{f=\pm 1} \left[\mathbf{u}_{Hf}(\mathbf{r}_\perp)\hat{a}_{Hf} + \mathbf{u}_{Vf}(\mathbf{r}_\perp)\hat{a}_{Vf}\right] e^{if\beta_0 z}, \tag{C5}$$

where $\mathbf{u}_{Hf/Vf}$ are the polarization vectors of the H/V guided modes with propagation direction parameter $f = \pm 1$.

Each of the four effective Hamiltonian $\hat{H}_{\mathrm{e}}^{ff'}$ terms in Equ. (C3) corresponds to the physics process with f'-propagating input field and f-propagating output field. For the case that only the forward-propagating fields are detected, the first two terms of the Hamiltonian yield the output we care about and the last two terms are losses. If the scattering among atoms can be ignored, then only the first term of the Hamiltonian is important. For now, we only consider the first term and ignore the propagation direction indexes f and f' as they both equal to 1.

We consider to rewrite the Hamiltonian in terms of the Stokes vector operators and the collective spin operators with the total atom number of N_A. We assume the photon number, N_L, is large and all atoms interact with the photon package indistinguishably in the measurement time period, τ, and interactions among atoms and the interference effect due to photon propagation are negligible crossing different measurement time steps. The total atomic angular momentum is $\mathbf{F} = \sum_i^{N_A} \mathbf{F}^{(i)}$.

The polarization state of the light can be represented on the Poincare sphere via Stokes vector $\mathbf{S}$. The quantized operators in the Schwinger representation with respect to the three Poincare sphere axes are defined as

$$\hat{S}_1 = \frac{1}{2}\left(\hat{a}_H^\dagger \hat{a}_H - \hat{a}_V^\dagger \hat{a}_V\right) \tag{C6}$$

$$\hat{S}_2 = \frac{1}{2}\left(\hat{a}_H^\dagger \hat{a}_V + \hat{a}_V^\dagger \hat{a}_H\right) \tag{C7}$$

$$\hat{S}_3 = \frac{1}{2i}\left(\hat{a}_H^\dagger \hat{a}_V - \hat{a}_V^\dagger \hat{a}_H\right) \tag{C8}$$

satisfying the $SU(2)$ algebra $[S_i, S_j] = i\varepsilon_{ijk}S_k$. The total photon number operator is defined as

$$\hat{S}_0 = \frac{1}{2}\left(\hat{a}_H^\dagger \hat{a}_H + \hat{a}_V^\dagger \hat{a}_V\right). \tag{C9}$$

Using these definitions in Equ. (C3), the effective Hamiltonian term can be rewritten as

$$\hat{H}_{e}^{f,f'=1} = \sum_F \hbar\chi_{0F} \sum_{F'} \frac{1}{1 + \delta_{F'}/\Delta_F + i\Gamma_{FF'}/2\Delta_F} \left[\hat{A}_0\hat{S}_0 + \hat{A}_1\hat{S}_1 + \hat{A}_2\hat{S}_2 + \hat{A}_3\hat{S}_3\right]. \qquad \text{(C10)}$$

We have written the detuning from a particular hyperfine transition as

$$\Delta_{F,F'} = \Delta_F + \delta_{F'} = \omega_0 - (\omega_F' - \omega_F), \qquad \text{(C11)}$$

where we have factored out the detuning relative to the largest hyperfine excited state under J' splittings,

$$\Delta_F \equiv \Delta_{F,F'_{\text{max}}} = \omega_0 - (\omega_{F'_{\text{max}}} - \omega_F), \qquad \text{(C12)}$$

and $\delta_{F'} \equiv \Delta_{F,F'} - \Delta_F$ is the residual detuning for the other hyperfine excited states. Correspondingly, for all $\Delta_{F,F'} \gg \Gamma_{FF'}$, the real part of the light shift interaction gives a coherent Hamiltonian of the form,

$$\hat{H}_{\text{coh}}^{f,f'=1} = \sum_F \hbar\chi_{0F} \sum_{F'} \frac{1}{1 + \delta_{F'}/\Delta_F} \left[\hat{A}_0\hat{S}_0 + \hat{A}_1\hat{S}_1 + \hat{A}_2\hat{S}_2 + \hat{A}_3\hat{S}_3\right]. \qquad \text{(C13)}$$

We have made the atomic operators that couple to the Stokes components at the atoms' positions, $\mathbf{r}' = (r'_\perp, \phi' = 0 \text{ or } \pi, z')$, are

$$\begin{aligned}
\hat{A}_0 =\ & C_{J'FF'}^{(0)} \left[|\mathbf{u}_H(\mathbf{r}'_\perp)|^2 + |\mathbf{u}_V(\mathbf{r}'_\perp)|^2\right] \hat{I}_F \\
& - 4C_{J'FF'}^{(1)} \text{Im}\left[u_z^*(r'_\perp)u_{r_\perp}(r'_\perp)\right] \hat{F}_\phi \\
& + 2C_{J'FF'}^{(2)} \text{Re}\left[u_z^*(r'_\perp)u_{r_\perp}(r'_\perp)\right] \left(\hat{F}_{r_\perp}\hat{F}_z + \hat{F}_z\hat{F}_{r_\perp}\right) \\
& + C_{J'FF'}^{(2)} \sum_i \left[|u_H^i(\mathbf{r}'_\perp)|^2 + |u_V^i(\mathbf{r}'_\perp)|^2\right] \left(\hat{F}_i^2 - \frac{1}{3}\hat{\mathbf{F}}\cdot\hat{\mathbf{F}}\right) \qquad \text{(C14a)}
\end{aligned}$$

$$\begin{aligned}
\hat{A}_1 =\ & C_{J'FF'}^{(0)} \left[|\mathbf{u}_H(\mathbf{r}'_\perp)|^2 - |\mathbf{u}_V(\mathbf{r}'_\perp)|^2\right] \hat{I}_F \\
& - 4C_{J'FF'}^{(1)} \text{Im}\left[u_z^*(r'_\perp)u_{r_\perp}(r'_\perp)\right] \hat{F}_\phi \\
& + 2C_{J'FF'}^{(2)} \text{Re}\left[u_z^*(r'_\perp)u_{r_\perp}(r'_\perp)\right] \left(\hat{F}_{r_\perp}\hat{F}_z + \hat{F}_z\hat{F}_{r_\perp}\right) \\
& + C_{J'FF'}^{(2)} \sum_i \left[|u_H^i(\mathbf{r}'_\perp)|^2 - |u_V^i(\mathbf{r}'_\perp)|^2\right] \left(\hat{F}_i^2 - \frac{1}{3}\hat{\mathbf{F}}\cdot\hat{\mathbf{F}}\right) \qquad \text{(C14b)}
\end{aligned}$$

$$\begin{aligned}
\hat{A}_2 =\ & 4C_{J'FF'}^{(1)} \left[\text{Re}\left(u_{r_\perp}^*(r'_\perp)u_\phi(r'_\perp)\right) \hat{F}_z - \text{Re}\left(u_\phi^*(r'_\perp)u_z(r'_\perp)\right) \hat{F}_{r_\perp}\right] \\
& + 2C_{J'FF'}^{(2)} \left[\text{Im}\left(u_{r_\perp}^*(r'_\perp)u_\phi(r'_\perp)\right) \left(\hat{F}_{r_\perp}\hat{F}_\phi + \hat{F}_\phi\hat{F}_{r_\perp}\right)\right. \\
& \qquad\qquad \left. + \text{Im}\left(u_\phi(r'_\perp)u_z^*(r'_\perp)\right) \left(\hat{F}_\phi\hat{F}_z + \hat{F}_z\hat{F}_\phi\right)\right] \qquad \text{(C14c)}
\end{aligned}$$

$$\hat{A}_3 = 4C^{(1)}_{J'FF'} \left[\text{Im} \left(u_{r_\perp}(r'_\perp) u^*_\phi(r'_\perp) \right) \hat{F}_z + \text{Im} \left(u_\phi(r'_\perp) u^*_z(r'_\perp) \right) \hat{F}_{r_\perp} \right]$$
$$+ 2C^{(2)}_{J'FF'} \left[\text{Re} \left(u^*_{r_\perp}(r'_\perp) u_\phi(r'_\perp) \right) \left(\hat{F}_{r_\perp} \hat{F}_\phi + \hat{F}_\phi \hat{F}_{r_\perp} \right) \right.$$
$$\left. + \text{Re} \left(u^*_\phi(r'_\perp) u_z(r'_\perp) \right) \left(\hat{F}_\phi \hat{F}_z + \hat{F}_z \hat{F}_\phi \right) \right]. \tag{C14d}$$

The dimensionless coupling constant,

$$\chi_{0F} = -\frac{2\pi\omega_0}{v_g \tau} \alpha(\Delta_F) = \frac{2\pi\omega_0}{v_g \tau} \frac{|d_{F'_{max}F}|^2}{\hbar \Delta_F} = n_g \sigma_0 \frac{\Gamma}{4\Delta_F} \tag{C15}$$

is a measure of the strength of the light-matter interaction. It is proportional to the detuning, Δ_F^{-1}, but more importantly to the ratio of the resonant atomic cross section, $\sigma_0 = 3\lambda_{FF'}^2/2\pi$, to the transverse mode area A. This ratio sets the strength of the single-atom coupling, as it roughly describes the amount of light scattered from the atom back into the probe mode.

For a psuedo-spin system, the spin operator $\mathbf{F} = \mathbf{J} = \sum_i^{N_A} \hat{\ } /2$ and satisfies the SU(2) symmetry that $[J_i, J_j] = i\epsilon_{ijk} J_k$ and hence, in Equs. (C14), the common factor $J_i J_j + J_j J_i = 2J_i J_j - i\epsilon_{ijk} J_k$.

Appendix D: Full Hamiltonian of Light-atom coupling

From Equ. (75), the effective Hamiltonian of the light-atom interaction can also be given by

$$H_e = \frac{2\pi\hbar\omega_0}{v_g \tau} \Big(\mathbf{u}^*_H(r'_\perp, \phi') \cdot \quad \cdot \mathbf{u}_H(r'_\perp, \phi') \hat{a}^\dagger_H \hat{a}_H + \mathbf{u}^*_V(r'_\perp, \phi') \cdot \quad \cdot \mathbf{u}_V(r'_\perp, \phi') \hat{a}^\dagger_V \hat{a}_V$$
$$+ \mathbf{u}^*_H(r'_\perp, \phi') \cdot \quad \cdot \mathbf{u}_V(r'_\perp, \phi') \hat{a}^\dagger_H \hat{a}_V + \mathbf{u}^*_V(r'_\perp, \phi') \cdot \quad \cdot \mathbf{u}_H(r'_\perp, \phi') \hat{a}^\dagger_V \hat{a}_H \Big). \tag{D1}$$

The atomic polarizability tensor   is composed of a dyad of vector dipole operators,

$$= -\frac{1}{\hbar} \sum_{F,F'} \frac{\mathbf{d}_{FF'} \mathbf{d}^\dagger_{F'F}}{\Delta_{FF'} + i\frac{}{2}} \tag{D2}$$

$$= \sum_{q,q'} \sum_{F,F'} \sum_{m_1,m_2,m'} \alpha_0(F,F') \mathbf{e}_q \otimes \mathbf{e}^*_{q'} |o^{J'F'}_{JF}|^2 C^{Fm_2;1q}_{F'm'} C^{Fm_1;1q'}_{F'm'} |Fm_2\rangle\langle Fm_1|, \tag{D3}$$

with the vector raising dipole operator,

$$\mathbf{d}^\dagger_{F'F} = \langle P_{J'}||d||S_{1/2}\rangle \sum_q \sum_{m,m'} \mathbf{e}^*_q o^{J'F'}_{JF} C^{Fm;1q}_{F'm'} |F'm'\rangle\langle Fm| \tag{D4}$$

where $o_{JF}^{J'F'}$ is the oscillator strength from Ref. [31] and $C_{F'm'}^{Fm;1q} \equiv \langle F'm'|Fm;1q\rangle$ is a Clebsch-Gordan coefficient. Notice that $m' = m_1 + q'$ and $m' = m_2 + q$ and thus

$$m_2 - m_1 = q - q'. \tag{D5}$$

The characteristic polarizability is

$$\alpha_0(F, F') = -\frac{|\langle P_{J'}||d||S_{1/2}\rangle|^2}{\hbar(\Delta_{F,F'} + i\frac{\Gamma}{2})} = -\frac{3\lambda_{J'}^3}{32\pi^3}\frac{\Gamma}{\Delta_{F,F'} + i\frac{\Gamma}{2}}. \tag{D6}$$

and the detuning is defined as

$$\Delta_{FF'} \equiv \omega - (\omega_{F'} - \omega_F). \tag{D7}$$

Due to the hyperfine ground splitting in Cs^{133} of approximately 9.2 GHz, the characteristic polarizabilities for the two ground hyperfine manifolds, Eq. (D6), can in general have different magnitudes and signs. Implied in the expression above is that we have chosen a J' transition - generally $S_{1/2} \to P_{1/2}$ (D_1) or $S_{1/2} \to P_{3/2}$ (D_2), which are separated by tens of THz and thus quite resolvable.

Now suppose that rather than using the magnetic sublevels within a single ground hyperfine state F as in Refs. [31], we begin with a dispersive interface defined on the $m = 0$ "clock" states between the $F = 3$ and $F = 4$ hyperfine states. To first order such states are insensitive to ambient magnetic field fluctuations. In the clock-state subspace, we designate the qubit states

$$|\uparrow\rangle \equiv |F = 4, m_F = 0\rangle \tag{D8}$$

$$|\downarrow\rangle \equiv |F = 3, m_F = 0\rangle. \tag{D9}$$

The light shift Hamiltonian, Eq. (D1), can then be expressed in this basis by finding the matrix elements between our relevant states. Since the atomic polarizability tensor is block-diagonal in the ground hyperfine states, we need only consider coupling between the states within the same manifold. For instance, we may have a $H - V$ mode crossing term like

$$\langle F, 0|\mathbf{u}_H^*(r'_\perp, \phi') \cdot \quad \cdot \mathbf{u}_V(r'_\perp, \phi')|F, 0\rangle$$

$$= \sum_{F'}\sum_{m'}\sum_{q,q'} \alpha_0(F, F')\big(\mathbf{e}_q \cdot \mathbf{u}_H^*(r'_\perp, \phi')\big)\big(\mathbf{e}_{q'}^* \cdot \mathbf{u}_V(r'_\perp, \phi')\big)|o_{JF}^{J'F'}|^2 C_{F'm'}^{F0;1q} C_{F'm'}^{F0;1q'} \tag{D10}$$

$$= \sum_{F'}\sum_{q} \alpha_0(F, F')\big(\mathbf{e}_q \cdot \mathbf{u}_H^*(r'_\perp, \phi')\big)\big(\mathbf{e}_q^* \cdot \mathbf{u}_V(r'_\perp, \phi')\big)|o_{JF}^{J'F'}|^2 C_{F'q}^{F0;1q} C_{F'q}^{F0;1q}. \tag{D11}$$

since $q + q' = 0$ and for the clock states $m' = q'$. By the nature of the nanofiber modes, if we choose V-mode polarization axis or the y-axis to be the quantization axis, then with the atoms positioned along the x-axis, the crossing term above always cancels. The same conclusion casts to other mode crossing terms. In fact, the conclusion above does not depend on the choice of basis. We can show that by rewriting the equations above as

$$\langle F, 0 | \mathbf{u}_H^*(r'_\perp, \phi') \cdot \quad \cdot \mathbf{u}_V(r'_\perp, \phi') | F, 0 \rangle$$

$$= \mathbf{u}_H^*(r'_\perp, \phi') \cdot \left[\sum_q \sum_{F'} \alpha_0(F, F') |o_{JF}^{J'F'}|^2 C_{F'q}^{F0;1q} C_{F'q}^{F0;1q} \mathbf{e}_q \mathbf{e}_q^* \right] \cdot \mathbf{u}_V(r'_\perp, \phi') \tag{D12}$$

$$= \mathbf{u}_H^*(r'_\perp, \phi') \cdot \quad^{F0;F0}] \cdot \mathbf{u}_V(r'_\perp, \phi') \tag{D13}$$

$$= \text{tr}\left[(\mathbf{u}_V(r'_\perp, \phi') \mathbf{u}_H^*(r'_\perp, \phi')) \cdot \quad^{F0;F0} \right], \tag{D14}$$

where $^{F0;F0} = \langle F, 0 | \quad | F, 0 \rangle = \sum_q \sum_{F'} \alpha_0(F, F') |o_{JF}^{J'F'}|^2 C_{F'q}^{F0;1q} C_{F'q}^{F0;1q} \mathbf{e}_q \mathbf{e}_q^*$ is the atomic polarizability tensor restricted to the $(F, m_F = 0)$ atomic space. The first block inside of the big bracket is a dyad. Obviously, the result as a trace does not depend on how we rotate the basis inside.

We stick to the choice of quantization axis used above, and have

$$H_{\text{e}} = \frac{\hbar}{\tau}\left(\chi_{H,\uparrow}|\uparrow\rangle\langle\uparrow| + \chi_{H,\downarrow}|\downarrow\rangle\langle\downarrow|\right)\hat{a}_H^\dagger \hat{a}_H$$

$$+ \frac{\hbar}{\tau}\left(\chi_{V,\uparrow}|\uparrow\rangle\langle\uparrow| + \chi_{V,\downarrow}|\downarrow\rangle\langle\downarrow|\right)\hat{a}_V^\dagger \hat{a}_V, \tag{D15}$$

where the coupling strengths are defined as

$$\chi_{H,\uparrow} = -\frac{2\pi\omega_0}{v_g}\langle F = 4, m = 0 | \mathbf{u}_H^*(r'_\perp, \phi') \cdot \quad \cdot \mathbf{u}_H(r'_\perp, \phi') | F = 4, m = 0 \rangle \tag{D16}$$

$$\chi_{H,\downarrow} = -\frac{2\pi\omega_0}{v_g}\langle F = 3, m = 0 | \mathbf{u}_H^*(r'_\perp, \phi') \cdot \quad \cdot \mathbf{u}_H(r'_\perp, \phi') | F = 3, m = 0 \rangle \tag{D17}$$

$$\chi_{V,\uparrow} = -\frac{2\pi\omega_0}{v_g}\langle F = 4, m = 0 | \mathbf{u}_V^*(r'_\perp, \phi') \cdot \quad \cdot \mathbf{u}_V(r'_\perp, \phi') | F = 4, m = 0 \rangle \tag{D18}$$

$$\chi_{V,\downarrow} = -\frac{2\pi\omega_0}{v_g}\langle F = 3, m = 0 | \mathbf{u}_V^*(r'_\perp, \phi') \cdot \quad \cdot \mathbf{u}_V(r'_\perp, \phi') | F = 3, m = 0 \rangle. \tag{D19}$$

To write down the Hamiltonian in the clock space,

$$\chi_{H,\uparrow/\downarrow} \equiv \chi_{H,F} = -\frac{2\pi\omega_0}{v_g}\langle F, 0 | \mathbf{u}_H^*(r'_\perp, \phi') \cdot \quad \cdot \mathbf{u}_H(r'_\perp, \phi') | F, 0 \rangle \tag{D20}$$

$$= -\frac{2\pi\omega_0}{v_g}\sum_{F'}\sum_q \alpha_0\left(F, F'\right)|\mathbf{e}_q \cdot \mathbf{u}_H^*(r'_\perp, \phi')|^2 |o_{JF}^{J'F'}|^2 |C_{F'q}^{F0;1q}|^2 \tag{D21}$$

$$\approx (\sigma_0 n_g) \sum_q \sum_{F'} \left(\frac{\Gamma}{4\left(\Delta_{F,F'} + i\Gamma/2\right)} \right) |\mathbf{e}_q \cdot \mathbf{u}_H^*(r'_\perp, \phi')|^2 |o_{JF}^{J'F'}|^2 |C_{F'q}^{F0;1q}|^2, \qquad \text{(D22)}$$

$$\chi_{V,\uparrow/\downarrow} \equiv \chi_{V,F} = -\frac{2\pi\omega_0}{v_g} \langle F, 0 | \mathbf{u}_V^*(r'_\perp, \phi') \cdot \quad \cdot \mathbf{u}_V(r'_\perp, \phi') | F, 0 \rangle \qquad \text{(D23)}$$

$$= -\frac{2\pi\omega_0}{v_g} \sum_{F'} \sum_q \alpha_0\left(F, F'\right) |\mathbf{e}_q \cdot \mathbf{u}_V^*(r'_\perp, \phi')|^2 |o_{JF}^{J'F'}|^2 |C_{F'q}^{F0;1q}|^2 \qquad \text{(D24)}$$

$$\approx (\sigma_0 n_g) \sum_q \sum_{F'} \left(\frac{\Gamma}{4\left(\Delta_{F,F'} + i\Gamma/2\right)} \right) |\mathbf{e}_q \cdot \mathbf{u}_V^*(r'_\perp, \phi')|^2 |o_{JF}^{J'F'}|^2 |C_{F'q}^{F0;1q}|^2, \qquad \text{(D25)}$$

$$\text{(D26)}$$

where we have approximated $\lambda_{J'} \approx \lambda = \frac{2\pi c}{\omega_0}$. We can also rewrite the result above in terms of dyadic Green functions and tensor polarizabilities as

$$\chi_{H,\uparrow/\downarrow} \equiv \chi_{H,F} = 4\pi k_0^2 \, \text{tr} \left\{ \text{Im} \left[\mathbf{G}_{HH}^*(\mathbf{r}'_\perp, \mathbf{r}'_\perp) \right] \cdot \quad^{F0;F0} \right\} \qquad \text{(D27)}$$

$$\chi_{V,\uparrow/\downarrow} \equiv \chi_{V,F} = 4\pi k_0^2 \, \text{tr} \left\{ \text{Im} \left[\mathbf{G}_{VV}^*(\mathbf{r}'_\perp, \mathbf{r}'_\perp) \right] \cdot \quad^{F0;F0} \right\}, \qquad \text{(D28)}$$

where

$$\mathbf{G}_{HH/VV}(\mathbf{r}', \mathbf{r}') = -\frac{i n_g}{2 k_0} \mathbf{u}_{H/V}(r'_\perp, \phi') \mathbf{u}_{H/V}^*(r'_\perp, \phi') \qquad \text{(D29)}$$

$$^{F0;F0} \approx \frac{\sigma_0 \lambda_{J'}}{4\pi^2} \sum_q \sum_{F'} \left(\frac{\Gamma}{4\left(\Delta_{F,F'} + i\Gamma/2\right)} \right) |o_{JF}^{J'F'}|^2 |C_{F'q}^{F0;1q}|^2 \mathbf{e}_q \mathbf{e}_q^*. \qquad \text{(D30)}$$

Appendix E: Junk: Effects of the evanescent field and the multilevel structure of the atom

In general,

$$\Gamma \propto \mathbf{d}_{eg} \cdot \text{Im} \left[\mathbf{G}^*(\mathbf{r}', \mathbf{r}') \right] \cdot \mathbf{d}_{eg}^* = \text{tr} \left[\mathbf{d}_{eg}^* \mathbf{d}_{eg} \cdot \text{Im} \left[\mathbf{G}^*(\mathbf{r}', \mathbf{r}') \right] \right] \propto \text{tr} \left[\quad_{eg} \cdot \text{Im} \left[\mathbf{G}^*(\mathbf{r}', \mathbf{r}') \right] \right] \qquad \text{(E1)}$$

where $_{eg}$ is the polarizability of the atom due to the transition between levels labeled by e and g. Therefore, the phase shift effect can be treated as a combined result of the atomic internal structure and the external field properties.

Since

$$\mathbf{d}_{eg} \cdot \text{Im} \left[\mathbf{G}^*(\mathbf{r}', \mathbf{r}') \right] \cdot \mathbf{d}_{eg}^* > 0 \qquad \text{(E2)}$$

for a physical decay rate, $\text{Im} \left[\mathbf{G}^*(\mathbf{r}', \mathbf{r}') \right]$ is positive definite and should always has three positive eigenvalues which indicate the range of Γ and phase shift at the atom position. The 3

corresponding eigenvectors indicate the 3 orthogonal principal axes of the radiation/emission surface. Case studies...

Radiation surface theory for the effective orientation of dipoles, elementary transitions (π and $\sigma_\pm$ transitions) and the example of completely mixed state case.

$$\Gamma_{mix} \propto \frac{1}{3}\mathrm{tr}\left[\mathrm{Im}\left[\mathbf{G}^*(\mathbf{r}', \mathbf{r}')\right]\right].\tag{E3}$$

For the atomic internal structure, we have the irreducible tensor decompositions that

$$_{eg} = {}^S + {}^V + {}^T.\tag{E4}$$

The scalar component will yield a decay rate equivalent to the completely mixed state case.

Another way to look at this problem is that we can decompose the guided mode Green function tensor into the scalar, vector and tensor parts as well, since the Green function tensor is reducible.

$$\mathbf{G}^g = \mathbf{G}^S + \mathbf{G}^V + \mathbf{G}^T.\tag{E5}$$

Therefore, where the position of the atom relative to the fiber mode yields a strong scalar component, the atomic response is more relatively independent of the atomic states...

Some interesting examples of state-dependent decay and phase shift...

---

[1] A Kuzmich, WP Bowen, AD Boozer, A Boca, CW Chou, L-M Duan, and HJ Kimble. Generation of nonclassical photon pairs for scalable quantum communication with atomic ensembles. *Nature*, 423(6941):731–734, 2003.

[2] Thibault Peyronel, Ofer Firstenberg, Qi-Yu Liang, Sebastian Hofferberth, Alexey V Gorshkov, Thomas Pohl, Mikhail D Lukin, and Vladan Vuletić. Quantum nonlinear optics with single photons enabled by strongly interacting atoms. *Nature*, 488(7409):57–60, 2012.

[3] DJ Alton, NP Stern, Takao Aoki, H Lee, E Ostby, KJ Vahala, and HJ Kimble. Strong interactions of single atoms and photons near a dielectric boundary. *Nature Physics*, 7(2):159–165, 2011.

[4] JD Thompson, TG Tiecke, NP de Leon, J Feist, AV Akimov, M Gullans, AS Zibrov, V Vuletić, and MD Lukin. Coupling a single trapped atom to a nanoscale optical cavity. *Science*, 340(6137):1202–1205, 2013.

[5] A. Goban, C.-L. Hung, S.-P. Yu, J. D. Hood, J. A. Muniz, J. H. Lee, M. J. Martin, A. C. McClung, K. S. Choi, D. E. Chang, O. Painter, and H. J. Kimble. Atom-Light Interactions in Photonic Crystals. *Nature communications*, 5(3808), #May# 2014.

[6] J Lee, DH Park, S Mittal, M Dagenais, and SL Rolston. Integrated optical dipole trap for cold neutral atoms with an optical waveguide coupler. *New Journal of Physics*, 15(4):043010, 2013.

[7] Ben Q. Baragiola, Leigh M. Norris, Enrique Montaño, Pascal G. Mickelson, Poul S. Jessen, and Ivan H. Deutsch. Three-dimensional light-matter interface for collective spin squeezing in atomic ensembles. *Phys. Rev. A*, 89:033850, Mar 2014.

[8] Fam Le Kien, V. I. Balykin, and K. Hakuta. Atom trap and waveguide using a two-color evanescent light field around a subwavelength-diameter optical fiber. *Phys. Rev. A*, 70:063403, Dec 2004.

[9] VI Balykin, K Hakuta, Fam Le Kien, JQ Liang, and M Morinaga. Atom trapping and guiding with a subwavelength-diameter optical fiber. *Physical Review A*, 70(1):011401, 2004.

[10] Kali Prasanna Nayak. *Optical Nanofibers for Manipulating Atoms and Photons*. PhD thesis, University of Electro-Communications, 2009.

[11] Kali P Nayak and K Hakuta. Single atoms on an optical nanofibre. *New Journal of Physics*, 10(5):053003, 2008.

[12] Jian Fu, Xiang Yin, Ningyuan Li, and Limin Tong. Atom waveguide and 1d optical lattice using a two-color evanescent light field around an optical micro/nano-fiber. *Chin. Opt. Lett.*, 6(2):112–115, Feb 2008.

[13] E. Vetsch, D. Reitz, G. Sagué, R. Schmidt, S. T. Dawkins, and A. Rauschenbeutel. Optical interface created by laser-cooled atoms trapped in the evanescent field surrounding an optical nanofiber. *Phys. Rev. Lett.*, 104:203603, May 2010.

[14] S. T. Dawkins, R. Mitsch, D. Reitz, E. Vetsch, and A. Rauschenbeutel. Dispersive optical interface based on nanofiber-trapped atoms. *Phys. Rev. Lett.*, 107:243601, Dec 2011.

[15] A. Goban, K. S. Choi, D. J. Alton, D. Ding, C. Lacroûte, M. Pototschnig, T. Thiele, N. P. Stern, and H. J. Kimble. Demonstration of a state-insensitive, compensated nanofiber trap. *Phys. Rev. Lett.*, 109:033603, Jul 2012.

[16] R Mitsch, C Sayrin, B Albrecht, P Schneeweiss, and A Rauschenbeutel. Quantum state-controlled directional spontaneous emission of photons into a nanophotonic waveguide. *Nature*

communications, 5, 2014.

[17] Peter Domokos, Peter Horak, and Helmut Ritsch. Quantum description of light-pulse scattering on a single atom in waveguides. *Phys. Rev. A*, 65:033832, Mar 2002.

[18] Fam Le Kien, S. Dutta Gupta, K. P. Nayak, and K. Hakuta. Nanofiber-mediated radiative transfer between two distant atoms. *Phys. Rev. A*, 72:063815, Dec 2005.

[19] Fam Le Kien, S Dutta Gupta, VI Balykin, and K Hakuta. Spontaneous emission of a cesium atom near a nanofiber: Efficient coupling of light to guided modes. *Physical Review A*, 72(3):032509, 2005.

[20] Fam Le Kien, V. I. Balykin, and K. Hakuta. Scattering of an evanescent light field by a single cesium atom near a nanofiber. *Phys. Rev. A*, 73:013819, Jan 2006.

[21] Jung-Tsung Shen and Shanhui Fan. Strongly correlated two-photon transport in a one-dimensional waveguide coupled to a two-level system. *Physical review letters*, 98(15):153003, 2007.

[22] Fam Le Kien and K. Hakuta. Cavity-enhanced channeling of emission from an atom into a nanofiber. *Phys. Rev. A*, 80:053826, Nov 2009.

[23] Manoj Das, A. Shirasaki, K. P. Nayak, M. Morinaga, Fam Le Kien, and K. Hakuta. Measurement of fluorescence emission spectrum of few strongly driven atoms using an optical nanofiber. *Opt. Express*, 18(16):17154–17164, Aug 2010.

[24] Fam Le Kien and K. Hakuta. Deterministic generation of a pair of entangled guided photons from a single atom in a nanofiber cavity. *Phys. Rev. A*, 84:053801, Nov 2011.

[25] D. Reitz, C. Sayrin, B. Albrecht, I. Mazets, R. Mitsch, P. Schneeweiss, and A. Rauschenbeutel. Backscattering properties of a waveguide-coupled array of atoms in the strongly nonparaxial regime. *Phys. Rev. A*, 89:031804, Mar 2014.

[26] F. Le Kien and A. Rauschenbeutel. Anisotropy in scattering of light from an atom into the guided modes of a nanofiber. *Physical Review A*, 90:023805, Aug 2014.

[27] R. Mitsch, C. Sayrin, B. Albrecht, P. Schneeweiss, and A. Rauschenbeutel. Exploiting the local polarization of strongly confined light for sub-micrometer-resolution internal state preparation and manipulation of cold atoms. *Phys. Rev. A*, 89:063829, Jun 2014.

[28] Philipp Schneeweiss, Fam Le Kien, and Arno Rauschenbeutel. Nanofiber-based atom trap created by combining fictitious and real magnetic fields. *New Journal of Physics*, 16(1):013014, 2014.

[29] J-B Béguin, EM Bookjans, SL Christensen, HL Sørensen, JH Müller, ES Polzik, and J Appel. Generation and detection of a sub-poissonian atom number distribution in a one-dimensional optical lattice. *Physical Review Letters*, 113(26):263603, 2014.

[30] A Kuzmich, L Mandel, and NP Bigelow. Generation of spin squeezing via continuous quantum nondemolition measurement. *Physical Review Letters*, 85:1594–1597, 2000.

[31] Ivan H. Deutsch and Poul S. Jessen. Quantum control and measurement of atomic spins in polarization spectroscopy. *Optics Communications*, 283(5):681 – 694, 2010. Quo vadis Quantum Optics?

[32] Brian Julsgaard, Jacob Sherson, J Ignacio Cirac, Jaromir Fiurášek, and Eugene S Polzik. Experimental demonstration of quantum memory for light. *Nature*, 432(7016):482–486, 2004.

[33] Kyung Soo Choi, Hui Deng, Julien Laurat, and HJ Kimble. Mapping photonic entanglement into and out of a quantum memory. *Nature*, 452(7183):67–71, 2008.

[34] M Hosseini, BM Sparkes, G Campbell, PK Lam, and BC Buchler. High efficiency coherent optical memory with warm rubidium vapour. *Nature communications*, 2:174, 2011.

[35] M Hosseini, Geoff Campbell, Ben M Sparkes, Ping K Lam, and Ben C Buchler. Unconditional room-temperature quantum memory. *Nature Physics*, 7(10):794–798, 2011.

[36] D V Vasilyev, K Hammerer, N Korolev, and A S Srensen. Quantum noise for faraday lightmatter interfaces. *Journal of Physics B: Atomic, Molecular and Optical Physics*, 45(12):124007, 2012.

[37] Gavin K. Brennen, Carlton M. Caves, Poul S. Jessen, and Ivan H. Deutsch. Quantum logic gates in optical lattices. *Phys. Rev. Lett.*, 82:1060–1063, Feb 1999.

[38] Vasily V Klimov and Martial Ducloy. Spontaneous emission rate of an excited atom placed near a nanofiber. *Physical Review A*, 69(1):013812, 2004.

[39] H Nha and W Jhe. Cavity quantum electrodynamics for a cylinder: inside a hollow dielectric and near a solid dielectric cylinder. *Physical Review A*, 56(3):2213, 1997.

[40] A. V. Maslov, M. I. Bakunov, and C. Z. Ning. Distribution of optical emission between guided modes and free space in a semiconductor nanowire. *Journal of Applied Physics*, 99(2):–, 2006.

[41] Roy J. Glauber and M. Lewenstein. Quantum optics of dielectric media. *Phys. Rev. A*, 43:467–491, Jan 1991.

[42] Thomas Søndergaard and Bjarne Tromborg. General theory for spontaneous emission in active dielectric microstructures: Example of a fiber amplifier, green function, green's function.

Physical Review A, 64(3):033812, 2001.

[43] Greg A Smith, Souma Chaudhury, and Poul S Jessen. Faraday spectroscopy in an optical lattice: a continuous probe of atom dynamics. *Journal of Optics B: Quantum and Semiclassical Optics*, 5(4):323, 2003.

[44] Clement Lacroûte, KS Choi, A Goban, DJ Alton, D Ding, NP Stern, and HJ Kimble. A state-insensitive, compensated nanofiber trap. *New Journal of Physics*, 14(2):023056, 2012.